Demonstration of mammalian protein *O*-mannosyltransferase activity: Coexpression of POMT1 and POMT2 required for enzymatic activity

Hiroshi Manya*, Atsuro Chiba[†], Aruto Yoshida[‡], Xiaohui Wang[§], Yasunori Chiba[§], Yoshifumi Jigami[§], Richard U. Margolis[¶], and Tamao Endo*[‖]

*Glycobiology Research Group, Tokyo Metropolitan Institute of Gerontology, Foundation for Research on Aging and Promotion of Human Welfare, Itabashi-ku, Tokyo 173-0015, Japan; [†]Department of Neurology, Kyorin University School of Medicine, Mitaka, Tokyo 181-8611, Japan; [‡]Central Laboratories for Key Technology, Kirin Brewery Company, Limited, Kanazawa-ku, Yokohama 236-0004, Japan; [§]Research Center for Glycoscience, National Institute of Advanced Industrial Science and Technology, Tsukuba, Ibaraki 305-8566, Japan; and [¶]Department of Pharmacology, New York University Medical Center, New York, NY 10016

Communicated by Armando J. Parodi, Fundacion Instituto Leloir, Buenos Aires, Argentina, November 6, 2003 (received for review September 4, 2003)

Defects in *O*-mannosylation of α-dystroglycan are thought to cause certain types of congenital muscular dystrophies with neuronal migration disorders. Among these muscular dystrophies, Walker–Warburg syndrome is caused by mutations in the gene encoding putative protein *O*-mannosyltransferase 1 (POMT1), which is homologous to yeast protein *O*-mannosyltransferases. However, there is no evidence that POMT1 has enzymatic activity. In this study, we first developed a method to detect protein *O*-mannosyltransferase activity in mammalian cells. Then, using this method, we showed that coexpression of both *POMT1* and *POMT2* (another gene homologous to yeast protein *O*-mannosyltransferases) was necessary for the enzyme activity, but expression of either *POMT1* or *POMT2* alone was insufficient. The requirement of an active enzyme complex of POMT1 and POMT2 suggests that the regulation of protein *O*-mannosylation is complex. Further, protein *O*-mannosylation appears to be required for normal structure and function of α-dystroglycan in muscle and brain. In view of the potential importance of this form of glycosylation for a number of developmental and neurobiological processes, the ability to assay mammalian protein *O*-mannosyltransferase activity should greatly facilitate progress in the identification and localization of *O*-mannosylated proteins and the elucidation of their functional roles.

Muscular dystrophies are genetic diseases that cause progressive muscle weakness and wasting (1, 2). The causative genes of several muscular dystrophies have been identified in the past 15 yr. The best known is the one described by Duchenne that results from mutations in the gene encoding a protein called dystrophin. Another subclass is congenital muscular dystrophies, where muscle weakness is apparent at birth or shortly afterward. Recent data suggest that aberrant protein glycosylation of a specific glycoprotein, α-dystroglycan (α-DG), is the primary cause of some forms of congenital muscular dystrophy (3, 4).

DG is encoded by a single gene and cleaved into two proteins, α- and β-DG, by posttranslational processing (5). In skeletal muscle, DG is a component of the dystrophin–glycoprotein complex. α-DG is an extracellular peripheral membrane glycoprotein anchored to the cell membrane by binding to β-DG, which is a transmembrane glycoprotein. The α-DG–β-DG complex is expressed in a broad array of tissues and is thought to act as a transmembrane linker between the extracellular matrix and intracellular cytoskeleton. This is because α-DG binds to laminin, and the intracellular domain of β-DG interacts with dystrophin in skeletal muscle (4, 6). α-DG is heavily glycosylated, and its sugars have a role in binding to laminin, neurexin, and agrin (4, 7, 8). We previously found that the glycans of α-DG include *O*-mannosyl oligosaccharides, and that a sialyl *O*-mannosyl glycan, Siaα2–3Galβ1–4GlcNAcβ1–2Man, is a laminin-binding ligand of α-DG (9). Mammalian *O*-mannosylation is an unusual type of protein modification that was first identified in chondroitin sulfate proteoglycans of brain (10–12) and is present in a limited number of glycoproteins of brain, nerve, and skeletal muscle (9, 13–17).

Muscle–eye–brain disease [MEB; Online Mendelian Inheritance in Man (OMIM) no. 253280] is an autosomal recessive disorder characterized by congenital muscular dystrophy, ocular abnormalities, and brain malformation (type II lissencephaly) (18). We previously reported that MEB is caused by mutations in the gene encoding *POMGnT1* (UDP-*N*-acetylglucosamine: protein *O*-mannose β1,2-*N*-acetylglucosaminyltransferase 1). *POMGnT1* is responsible for the formation of the GlcNAcβ1–2Man linkage of *O*-mannosyl glycan, and all mutations cause a loss of enzyme activity (19–21). Like MEB, Fukuyama-type congenital muscular dystrophy (FCMD; OMIM no. 253800) (22) and Walker–Warburg syndrome (WWS; OMIM no. 236670) (23) are autosomal recessive disorders characterized by congenital muscular dystrophy, lissencephaly, and eye anomalies. FCMD and WWS are caused by mutations in the genes *fukutin* (24) and protein *O*-mannosyltransferase 1 (*POMT1*) (25). *POMT1* encodes a protein that is homologous to members of the family of protein *O*-mannosyltransferases (PMTs, in vertebrates named POMTs) in yeast (26). In yeast, PMTs catalyze the transfer of a mannosyl residue from dolichyl phosphate mannose (Dol-P-Man) to Ser/Thr residues of certain proteins (27). However, in mammals, there is no evidence that POMT1 has this activity, and its function remains unknown. The function of fukutin is also unknown, although an analysis of its sequence predicts that it is involved in modifying cell surface glycans (28).

Recently, 20% of WWS patients (6 of 30 unrelated WWS cases) were found to have mutations in *POMT1*. *POMT1* is highly expressed in fetal brain, testis, and skeletal muscle (26), which are the tissues affected in WWS. It is noteworthy that none of the 30 cases studied had mutations in another homologue, *POMT2*, which is 33% identical to *POMT1* (25, 29). POMT2 was found not to have POMT activity (29). Thus, POMT activity of POMTs has not yet been detected in vertebrates. Determining whether POMT1 is involved in the biosynthesis of *O*-mannosyl glycans will help in understanding the relationship between protein *O*-mannosylation and congenital muscular dystrophies with brain malformation.

In this study, we developed a method to detect the enzymatic activity of POMT in mammalian cells and tissues. Using this method, we examined whether POMT activity is encoded by the

Abbreviations: DG, dystroglycan; Dol-P-Man, dolichyl phosphate mannose; FCMD, Fukuyama-type congenital muscular dystrophy; MEB, muscle–eye–brain disease; PMT and POMT, protein *O*-mannosyltransferase; WWS, Walker–Warburg syndrome.

[‖]To whom correspondence should be addressed. E-mail: endo@tmig.or.jp.

www.pnas.org/cgi/doi/10.1073/pnas.0307228101

POMT1 gene and/or the *POMT2* gene after expression of POMT1, POMT2, or both. We found that POMT activity was significantly increased in cells cotransfected with both *POMT1* and *POMT2* but not in cells transfected with *POMT1* or *POMT2* alone.

Methods

Construction of Expression Plasmids. Human cDNAs encoding *POMT1* (26) and *POMT2* (29) were obtained by RT-PCR and 5′-RACE. RT-PCR was carried out by an Access RT-PCR kit (Promega) with brain total RNA (Clontech). 5′-RACE was carried out by nested PCR by using Human Brain and Kidney Marathon-Ready cDNAs (Clontech). The *myc*-tag sequence (GGPEQKLISEEDLNS) was fused to the C terminus of *POMT1*. DNA sequences were confirmed by an ABI PRISM 377 DNA sequencer (Perkin–Elmer Japan, Yokohama, Japan) with the Thermo Sequenase II Dye Terminator Cycle Sequence kit (Amersham Pharmacia Biosciences). The cDNAs encoding *POMT1-myc* and *POMT2* were inserted into a mammalian expression vector, pcDNA3.1 Zeo(−) (Invitrogen) and pcDNA3.1 Hygro(+) (Invitrogen), respectively.

Using NETOGLYC 2.0 (www.cbs.dtu.dk/services/NetOGlyc), we predicted that potential *O*-glycosylation sites of α-DG are clustered in the region corresponding to amino acids 313–483 (30). This region does not have any potential *N*-glycosylation sites. We amplified this region from mouse genomic DNA by PCR by using the primer set 5′-GGGAATTCCACGCCACAC-CTACAC-3′ (sense) and 5′-GGGTCTAGAACTGGTGG-TAGTACGGATTCG-3′ (antisense) and subcloned it into the pGEX-4T-3 vector to express the peptide as a GST-fusion protein (Amersham Pharmacia Biosciences). The correctness of the subcloned sequence was confirmed by DNA sequencing.

Preparation of GST-α-DG. BL21(DE3) *Escherichia coli* cells were transformed with the expression plasmid of GST-α-DG. Cultures were grown at 37°C to $A620 = 0.5$. At this point, 1 mM isopropyl-D-thiogalactopyranoside was added to the culture to induce GST-α-DG expression. The induced cells were grown in parallel for an additional 4 h at 37°C, harvested by centrifugation at 6,000 × *g* for 15 min at 4°C, suspended in 10 ml of PBS, pH 7.4, and broken with a tip-type sonicator. The cell supernatant was recovered by ultracentrifugation at 100,000 × *g* for 1 h, loaded onto a glutathione-Sepharose column (GSTrap, 1 ml, Amersham Pharmacia Biosciences), and washed with PBS. The absorbed recombinant GST-α-DG proteins were eluted with 10 mM reduced glutathione in PBS at a flow rate of 1 ml/min and dialyzed with 50 mM $(NH_4)HCO_3$, pH 7.0. Protein concentration was determined by BCA assay (Pierce), and the purity of GST-α-DG was confirmed by SDS/PAGE visualized with Coomassie brilliant blue R-250 and by Western blotting with anti-GST mAb (GST-2) (Sigma–Aldrich).

Cell Culture and Preparation of Cell Extracts. Human embryonic kidney 293T (HEK293T) cells were maintained in DMEM (Invitrogen) supplemented with 10% FBS (Invitrogen)/2 mM L-Gln/100 units/ml penicillin/50 μg/ml streptomycin at 37°C with 5% CO_2. The cells were homogenized in 10 mM Tris·HCl, pH 7.4/1 mM EDTA/250 mM sucrose/1 mM DTT, with a protease inhibitor mixture (3 μg/ml pepstatin A/1 μg/ml leupeptin/1 mM benzamidine-HCl/1 mM PMSF). After centrifugation at 900 × *g* for 10 min, the supernatant was subjected to ultracentrifugation at 100,000 × *g* for 1 h. The precipitate was used as the microsomal membrane fraction. Protein concentration was determined by BCA assay.

Expression of Human *POMT1* and *POMT2*. The expression plasmids of human pcDNA3.1-*POMT1-myc* and pcDNA3.1-*POMT2* were transfected into HEK293T cells by using LipofectAMINE PLUS reagent (Invitrogen), according to the manufacturer's instructions. The transfected cells were cultured for 3 days in complete medium, harvested, and homogenized.

Antibodies and Western Blot Analysis. Rabbit antiserum specific to the human POMT2 was produced by using a synthetic peptide corresponding to residues 390–403 (HNTNSDPLDPSFPV) of POMT2. A Cys residue was added to the N terminus of the POMT2 synthetic peptide (390–403 aa), so that the antigenic peptide could be conjugated to keyhole limpet hemocyanin (KLH). Rabbits were immunized with the antigenic peptide-KLH conjugate. Anti-myc mAb was purchased from Invitrogen. The microsomal fractions (20 μg) were separated by SDS/PAGE (10% gel), and proteins were transferred to a poly(vinylidene difluoride) membrane. The membrane, after blocking in PBS containing 5% skim milk and 0.5% Tween 20, was incubated with each Ab, and then the membrane was treated with anti-rabbit or anti-mouse IgG conjugated with horseradish peroxidase (Amersham Pharmacia Biosciences). Proteins bound to Ab were visualized with an enhanced chemiluminescence kit (Amersham Pharmacia Biosciences).

Assay for POMT Activity. Assays for POMT activity were carried out in a 20-μl reaction volume containing 20 mM Tris·HCl (pH 8.0), 100 nM Dol-P-[^{3}H]Man (125,000 dpm/pmol) (American Radiolabeled Chemicals, St. Louis), 2 mM 2-mercaptoethanol, 10 mM EDTA, 0.5% *n*-octyl-β-D-thioglucoside (DOJINDO, Kumamoto, Japan), 10 μg of GST-α-DG, and 80 μg of microsomal membrane fraction. The reaction was initiated by adding the protein extract. After 1-h incubation at 28°C, the reaction was stopped by adding 200 μl of PBS containing 1% Triton X-100, and the reaction mixture was centrifugated at 10,000 × *g* for 10 min. The supernatant was removed, mixed with 400 μl of PBS containing 1% Triton X-100 and 10 μl of glutathione-Sepharose 4B beads (Amersham Pharmacia Biosciences), rotated at 4°C for 1 h, and washed three times with 20 mM Tris·HCl (pH 7.4) containing 0.5% Triton X-100. The radioactivity adsorbed to the beads was measured by using a liquid scintillation counter. The incorporation of radioactive mannose into GST-α-DG was detected by SDS/PAGE and subsequent autoradiography.

To characterize the linkage of the mannosyl residue, the radioactive products absorbed to the glutathione-Sepharose beads were incubated with jack bean-α-mannosidase (0.8 units) (Seikagaku, Tokyo) in 50 μl of 0.1 M ammonium acetate buffer (pH 4.5) containing 1 mM $ZnCl_2$ at 37°C. Jack bean-α-mannosidase (0.8 units) was added freshly every 24 h and incubated for up to 60 h. Inactivated jack bean-α-mannosidase, prepared by heating the enzyme (100°C, 5 min), was used a control. After incubation, the radioactivities of the supernatant and the beads were measured by using a liquid scintillation counter.

Results

Detection of Transferase Activity of Mannose from Dol-P-Man to GST-α-DG. Initially, we attempted to detect mannose transferase activity based on an assay for POMT activity in yeast using several synthetic peptides and Triton X-100 as a detergent (31, 32). However, we did not detect any activity in several mammalian tissues and cells, possibly due to the specificity of the acceptor peptide sequence. If the enzyme recognizes a specific amino acid sequence, α-DG may be a suitable acceptor, because α-DG has *O*-mannosyl glycan (9, 17). Therefore, we prepared a GST fusion protein of α-DG (GST-α-DG) for a candidate acceptor by using an *E. coli* expression system. However, using the GST-α-DG as an acceptor and the Dol-P-Man as a donor substrate, we still did not observe any enzymatic activity. Next, we examined the effect of detergent because yeast PMTs were integral membrane proteins and thus hydrophobic proteins (27).

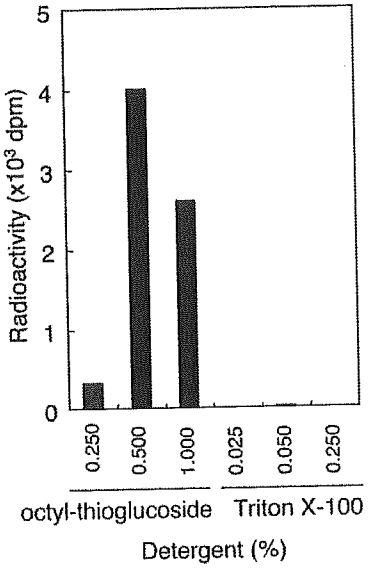

Fig. 1. Effect of detergents on POMT activity. POMT activity was measured in a 20-μl reaction volume containing 20 mM Tris·HCl (pH 8.0), 100 nM Dol-P-[^{3}H]Man (125,000 dpm/pmol), 2 mM 2-mercaptethanol, 10 mM EDTA, 10 μg of GST-α-DG, and 80 μg of HEK293T cell microsomal membrane fraction in the presence of *n*-octyl-β-D-thioglucoside or Triton X-100. The reaction was initiated by adding the protein extract and continued at 28°C for 1 h. After incubation, GST-α-DG was separated by glutathione-Sepharose beads and then the incorporated [^{3}H]Man to GST-α-DG was measured with a liquid scintillation counter.

Because Triton X-100 is a nonionic detergent, we examined several ionic and ampholytic detergents, including alkylglycosides. We found that *n*-octyl-β-D-thioglucoside was most effective, and its optimal concentration was 0.5% (wt/vol) (Fig. 1). Accordingly, 0.5% of *n*-octyl-β-D-thioglucoside was used in the following enzyme assays.

Next, we confirmed that a mannose residue was transferred from Dol-P-Man to GST-α-DG. As shown in Fig. 2*A*, the radioactivity of [^{3}H]Man was incorporated into the glutathione-Sepharose beads in the presence of both the membrane fraction and an acceptor (lane 2), but the radioactivity was not incorporated without the membrane fraction (lane 1) or without the acceptor (lane 3). GST-α-DG eluted from the glutathione-Sepharose beads was detected as triplet bands at ≈50 kDa in the presence or absence of the membrane fraction by SDS/PAGE (Fig. 2*B*). Because all bands were stained with the anti-GST Ab, the largest molecular-weight band was thought to be the full-length GST-α-DG, and the smaller bands were probably fragments of degraded GST-α-DG. We observed significant incorporation of radioactive mannose into all GST-α-DGs in the presence of the membrane fraction (Fig. 2*C*, lane 2). No radioactivity was observed when GST-α-DG was incubated with GDP-[^{3}H]Man instead of Dol-P-[^{3}H]Man. Based on these results, we concluded that the mannose donor was Dol-P-Man and not GDP-Man.

POMT Activity of Human POMT1 and POMT2. The mammalian *POMT1* and *POMT2* genes are thought to encode POMTs, because they are homologs of yeast *O*-mannosyltransferases (*PMT*s) (26, 29). However, attempts to show that mammalian POMT1 and/or POMT2 has POMT activity have so far been unsuccessful. To demonstrate the POMT activities of POMT1 and POMT2, we constructed the expression plasmids pcDNA3.1-*POMT1myc* and pcDNA3.1-*POMT2*, which express POMT1 tagged with the *myc* epitope (POMT1myc) and POMT2, respectively. These two plasmids were transfected individually or simultaneously into HEK293T cells, and then we recovered the microsomal membrane fraction from the transfected cells. A Western blot analysis using an anti-myc Ab and anti-POMT2 antiserum revealed POMT1myc and the POMT2 at ≈75 kDa in the membrane fraction of each type of transfected

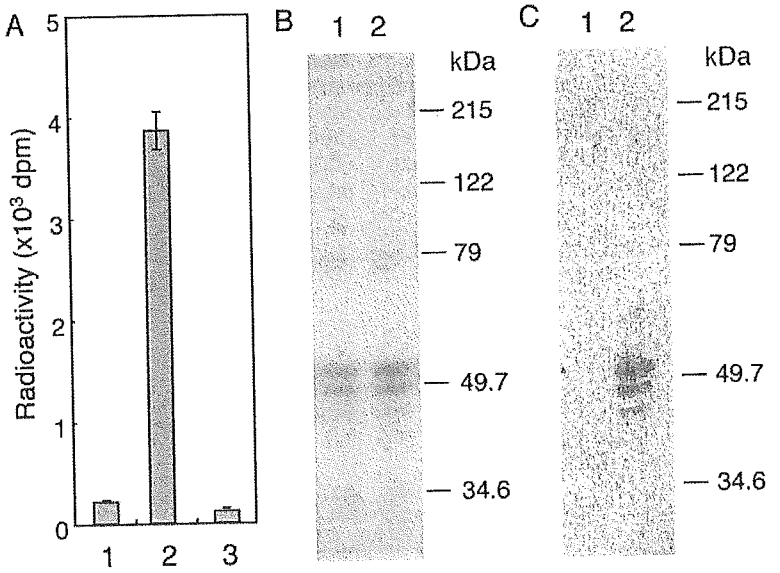

Fig. 2. POMT activity in HEK293T cells. (*A*) Incorporation of [^{3}H]Man into GST-α-DG. Lane 1, incubation with GST-α-DG but without membrane fraction; lane 2, incubation with membrane fraction and GST-α-DG; lane 3, incubation with membrane fraction but without GST-α-DG. (*B*) After incubation, a reaction mixture of lane 1 or 2 in *A* was subjected to SDS/PAGE (10% gel) and was stained by Coomassie. Lane 1, corresponds to lane 1 of *A*, and lane 2 corresponds to lane 2 of *A*. (*C*) Autoradiography of *B*. POMT activity was based on the rate of mannose transfer to GST-α-DG using the membrane fractions from HEK293T cells. The products were recovered by the glutathione-Sepharose beads. Incorporation of [^{3}H]Man into GST-α-DG was measured with a liquid scintillation counter. Molecular mass standards are shown to the right of *B* and *C*.

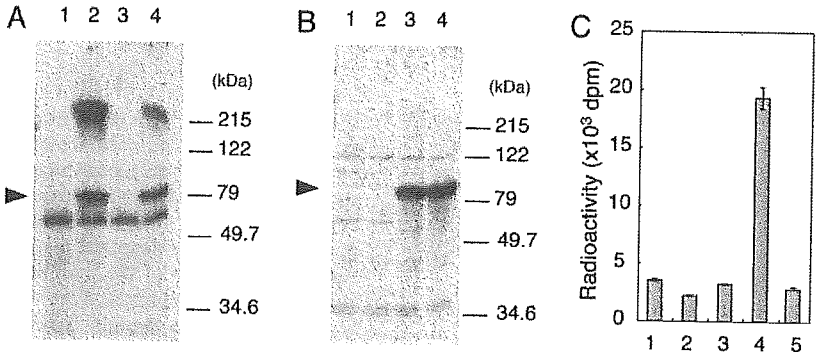

Fig. 3. POMT activity of human POMT1 and POMT2. Western blot analyses of myc-tagged POMT1 (*A*) and POMT2 (*B*) expressed in HEK293T cells. Lanes 1, cells transfected with vector alone; lanes 2, cells transfected with human *POMT1*; lanes 3, cells transfected with human *POMT2*; lanes 4, cells cotransfected with *POMT1* and *POMT2*. The proteins (20 μg of HEK293T cell microsomal membrane fraction) were subjected to SDS/PAGE (10% gel), and the separated proteins were transferred to a poly(vinylidene difluoride) (PVDF) membrane. The PVDF membrane was stained with anti-myc (*A*) or anti-POMT2 Ab (*B*). Molecular mass standards are shown to the right of *A* and *B*. (*C*) POMT activity of membrane fractions from each of these four types (lanes 1–4) plus a mixture of the membrane fractions from the *POMT1*-transfected cells and *POMT2*-transfected cells (lane 5).

cells (Fig. 3 *A* and *B*). The band at ≈60 kDa in Fig. 3*A* was a nonspecific band. We assessed the POMT activity by using these membrane fractions as an enzyme source. Because HEK293T cells had endogenous POMT activity (Fig. 2*A*, lane 2), we assumed that the activity in the mock-transfected cells (Fig. 3*C*, lane 1, transfected with a vector alone) was the background of this assay. The POMT activity was significantly increased in the cells cotransfected with *POMT1* and *POMT2* (Fig. 3*C*, lane 4) but was not increased in the cells transfected with either *POMT1* or *POMT2* alone (Fig. 3*C*, lanes 2 and 3). These results clearly show that the human POMT1 and/or POMT2 have POMT activity, and the expression of enzymatic activity requires both POMT1 and POMT2. It is probable that a heterophilic interaction between POMT1 and POMT2 is involved in the formation of the active enzyme. It is noteworthy that the POMT activity in a mixture of the membrane fractions from the *POMT1*- and *POMT2*-transfected cells was similar to the background level (Fig. 3*C*, lane 5). This suggests that the complex between POMT1 and POMT2 is formed during the synthesis of POMT1 and POMT2.

Temperature had a dramatic effect on the rate of the reaction, and the enzyme had an optimal temperature ≈22°C (Fig. 4*A*). The lower reaction rate above 30°C is probably due to lability of the enzyme at higher temperatures. At this point, it is unclear why the enzyme activity shows this temperature lability. Degradation of enzymes and acceptor proteins during incubation is probably not the cause, because POMT1, POMT2, and GST-α-DG were not degraded significantly during incubation, and the same temperature–activity relationships were seen even at short incubation times of 5–30 min (Fig. 4*A Inset*). It is possible that the observed temperature lability is due to dissociation of a stabilizing protein from the enzyme–acceptor complex during incubation, or to a temperature-dependent change in the detergent effects. The optimal pH of the POMT activity of POMT1 and POMT2 was ≈8.5 (Fig. 4*B*). Most of the glycosyltransferases studied to date require divalent cations as activators (33). In previous yeast PMT assays (31, 32), Mg^{2+} (7~8 mM) was present in the reaction mixture. Among the divalent metal ions examined in the present study, Mg^{2+} showed slightly to activate POMT (Fig. 4*C*). The enzyme was fully active in the presence of 10 mM EDTA. Both Ca^{2+} and Mn^{2+} suppressed the enzyme activity. Taken together, human POMT did not require a divalent cation for its activity.

Identification of Product by POMT Products. Digestion of [^{3}H]mannosyl-GST-α-DG by jack bean α-mannosidase, which cleaves the Manα1-Ser/Thr linkage (32), released the radioactivity from the GST-α-DG and decreased the radioactivity remaining in the GST-α-DG (on the beads) (Fig. 5). The release of radioactivity increased with increasing concentration of α-mannosidase. The

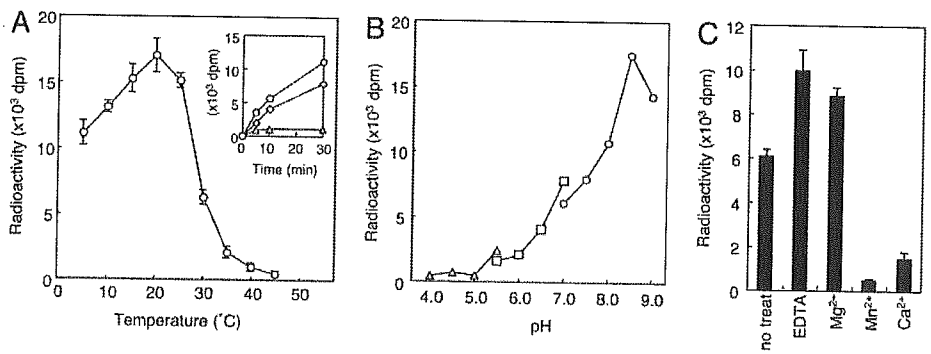

Fig. 4. Dependence of POMT activity of human POMT1 and POMT2 on temperature (*A*), pH (*B*), and various divalent cations and EDTA (*C*). (*A*) The temperature–activity relationships at short incubation times (5–30 min) are shown (*Inset*). Squares, 15°C; circles, 25°C; triangles, 35°C. (*B*) Triangles, squares, and circles indicate sodium acetate buffer (pH 4.0~5.5), Mes buffer (pH 5.5~7.0), and Tris·HCl buffer (pH 7.0~9.0), respectively. (*C*) The enzyme was assayed with various divalent cations at 10 mM or EDTA at 10 mM. The presence of Mg^{2+} had a slight enhanced effect on the activity. The enzyme was fully active in the presence of EDTA. Mn^{2+} and Ca^{2+} suppressed the enzyme activity. Eighty micrograms of HEK293T cell microsomal membrane protein was used for each assay.

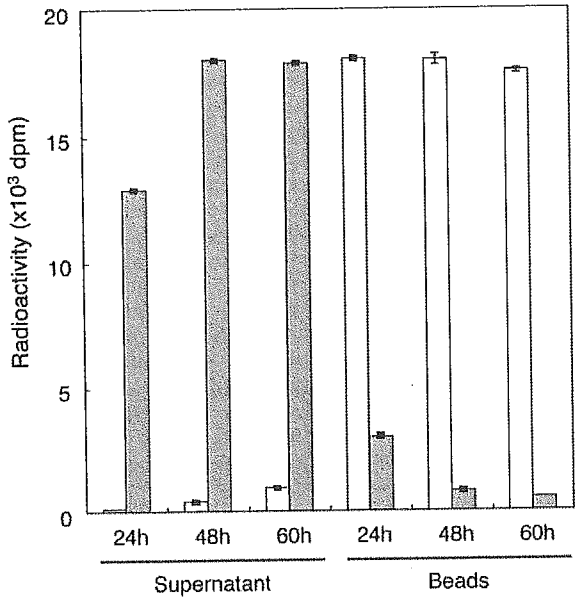

Fig. 5. α-Mannosidase digestion of mannosyl-GST-α-DG. Glutathione-Sepharose beads bearing [^{3}H]mannosyl-GST-α-DG were incubated with jack bean α-mannosidase. At 24-h incubation, 0.8 unit of enzyme was added at 0 h; at 48-h incubation, 0.8 unit of enzyme was added at 0 and 24 h; and at 60-h incubation, 0.8 unit of enzyme was added at 0, 24, and 48 h. After incubation and centrifugation, the radioactivities of the supernatant and the beads were measured with a liquid scintillation counter. Filled bars, active α-mannosidase; open bars, inactive (heat-treated) α-mannosidase. The radioactivity released to the supernatant increased with increasing amount of α-mannosidase used, and the radioactivity remained on the beads decreased correspondingly.

radioactivity was not released by treatment with heat-inactivated α-mannosidase (Fig. 5). Heat-inactivated α-mannosidase treatment confirmed that the GST-α-DG was not eluted spontaneously from the glutathione-Sepharose beads during treatment with the α-mannosidase (data not shown). These results indicate that a mannose residue is linked to a Ser or a Thr in the GST-α-DG by an α-*O*-glycosidic linkage and not by a β-*O*-glycosidic linkage.

Discussion

Protein *O*-mannosylation is catalyzed by a family of POMTs (PMTs), which were first characterized in the yeast *Saccharomyces cerevisiae* (27). Two human homologues of *PMT* (*POMT1* and *POMT2*) were found (26, 29), but their gene products did not show any POMT activity.

We first tried to develop an assay method to detect POMT activity in mammalian tissues and cells using the method for assaying yeast-like POMT activity *in vitro*. We did not detect any enzymatic activity when we used different organs, tissues, and cultured cells as an enzyme source; Dol-P-Man or GDP-Man as the sugar donor; Triton X-100 as a detergent; and various synthetic peptides as the acceptor. One possible reason for the lack of activity is that mammalian POMT might recognize an amino acid sequence different from the one recognized by the yeast enzyme. Another possible reason is that the hydrophobicity of the mammalian enzyme might be different from that of the yeast enzyme. Therefore, we thought that α-DG might be a suitable acceptor, because it is an *O*-mannosylated protein in mammals (9, 14, 15, 17). Therefore, we used a GST fusion protein of α-DG (GST-α-DG) instead of synthetic peptides for the acceptor and detergents other than Triton X-100. With these changes, we succeeded in detecting mammalian POMT activity. The best detergent under our experimental conditions was *n*-octyl-β-D-thioglucoside (Fig. 1).

Using the assay method, mammalian POMT was found to catalyze a yeast-like *O*-mannosyl transfer reaction. It transfers a mannosyl residue from Dol-P-Man (not from GDP-Man) to Ser/Thr residues of target proteins, and it is localized in endoplasmic reticulum (27). Mammalian POMT may require a specific amino acid sequence or protein conformation for activity, because synthetic peptides ranging in length from 3 to 10 aa [e.g., 316–325(ATPTPVTAIG), 366–368(PTV)] from potential *O*-glycosylation sites of human α-DG, 313–483 did not serve as acceptors even using *n*-octyl-β-D-thioglucoside. It may be relevant that *O*-mannosylated glycoprotein is abundant in yeast cell walls but is unusual and limited in mammals (17, 27, 34). The requirement for a different detergent for the mammalian enzyme may be due to the different lipid composition in yeast and mammalian membranes.

Using this method, we demonstrated that human POMT1 and/or POMT2 have POMT activity, but only when they are coexpressed, suggesting that POMT1 and POMT2 form a heterocomplex to express enzymatic activity. Because yeast PMT1 and PMT2 form a heterocomplex, and this complex formation is essential for maximal POMT activity (35, 36), the complex in mammals may be similar to the complex in yeast. However, attempts to detect this complex after solubilization of membrane proteins using various detergents or a mixture of detergents, followed by immunoprecipitation with Abs to myc, POMT1, and POMT2 were unsuccessful. Why expression of POMT1 or POMT2 alone did not result in POMT activity is unclear. One possibility is that POMT1 and POMT2 cannot form a homocomplex. Another possibility is that a homocomplex of POMT1 or POMT2 does not have enzymatic activity. In HEK293T cells transfected with the *POMT1* gene, the broad band seen above 215 kDa (Fig. 3*A*, lanes 2 and 4) probably represents POMT1 protein aggregates resulting from its overexpression, because there is no evidence for the presence of POMT2 protein migrating at this position (see Fig. 3*B*, lanes 3 and 4). *POMT1* and *POMT2* are expressed in all human tissues, but *POMT1* is highly expressed in fetal brain, testis, and skeletal muscle, and *POMT2* is predominantly expressed in testis (26, 29). *O*-Mannosylation seems to be uncommon in mammals, and only a few *O*-mannosylated proteins have been identified (17). It will be of interest to determine the regulatory mechanisms for protein *O*-mannosylation in each tissue. Future studies are needed to clarify the distribution of *O*-mannosyl glycans and of *O*-mannosylated glycoproteins in various mammalian tissues.

WWS and MEB are clinically similar autosomal recessive disorders characterized by congenital muscular dystrophy, lissencephaly, and eye anomalies, but WWS is a more severe syndrome than MEB (23, 37). Patients with WWS are severely affected from birth (brain malformation is particularly common), and few live beyond infancy. In MEB, the cerebral and ocular anomalies are also severe, but some patients reach adulthood (18, 37). The present results may explain the difference of severity between the two diseases. If POMGnT1, which is responsible for the formation of the GlcNAcβ1–2Man linkage of *O*-mannosyl glycans (19), is nonfunctional, only *O*-mannose residues may be present on α-DG in MEB. On the other hand, *POMT1* mutations cause complete loss of *O*-mannosyl glycans in WWS. Because *O*-mannosyl glycans have several peripheral structures [Siaα2–3Galβ1–4GlcNAcβ1–2Man, Galβ1–4(Fucα1–3)GlcNAcβ1–2Man, and HSO_3-3GlcAβ1–3Galβ1–4GlcNAcβ1–2Man] (17), none of these *O*-mannosyl glycans can be formed if either POMGnT1 or POMT1 does not function. Because these structures play an important role in adhesive processes, a defect in the biosynthesis of *O*-mannosyl glycans may have a severe effect on cell migration and cell adhesion. It is possible that attachment of a single mannose residue on α-DG in

MEB is responsible for the difference in clinical severity of WWS and MEB.

Recently, 6 of 30 WWS patients were found to have mutations in *POMT1*, whereas none had mutations in *POMT2* (25). A possible explanation for the absence of *POMT2* mutations in human subjects is that *POMT2* may be essential for normal development; i.e., *POMT2* mutations may be embryonic-lethal. Another possibility is that patients with *POMT2* mutations were simply not included in the 30 WWS patients. A worldwide survey of the occurrence of *POMT2* mutations is needed to determine whether WWS is caused by *POMT* mutations. The *rt* mutation in *Drosophila*, which causes defects of myogenesis, was found to be due to a mutation in a homologue of *POMT1* (29, 38). The mutation also causes reduced fertility and reduced viability. Although the *rt* gene product is not known to initiate the biosynthesis of *O*-mannosyl glycans, *O*-mannosylation is an evolutionarily conserved protein modification and may be essential for muscle development in both vertebrates and invertebrates.

The skeletal muscle of patients with WWS, MEB, and FCMD was found to be deficient in highly glycosylated α-DG, whereas β-DG and laminin α2 were normally expressed (3, 7, 25, 39, 40). Additionally, defective glycosylation of α-DG has been implicated in congenital muscular dystrophy type 1C (MDC1C). The defective glycosylation is caused by mutations in a gene encoding a putative glycosyltransferase (FKRP, fukutin-related protein) (41). The gene *large*, which is mutated in the myodystrophy (*myd*) mouse, encodes a putative glycosyltransferase (42). α-DG in the muscle and brain of *myd* mice, like that of WWS, MEB, and FCMD patients, was found to be hypoglycosylated. Moreover, hypoglycosylated α-DG in the muscle membranes of MEB and FCMD patients and the *myd* mouse has greatly reduced affinities for laminin, neurexin, and agrin (8). In other words, interference in *O*-mannosylation of α-DG may lead to a combination of muscle, eye, and brain abnormalities and is a previously undescribed pathomechanism for muscular dystrophy as well as neuronal migration disorder. Some forms of muscular dystrophy may be due to defects of glycosyltransferases, but the substrates of these enzymes, with the exception of POMGnT1 (19) and POMT1 (this study), are largely unknown. Because FKRP and fukutin are thought to be Golgi-resident proteins (43), it is possible that defects of these proteins cause abnormal processing of α-DG. Identification and characterization of each enzyme will help reveal the molecular pathomechanisms of congenital muscular dystrophies that are accompanied by brain malformation. Because only 20% of WWS patients were found to have mutations in *POMT1* (25), other as-yet-unidentified genes may be responsible for this syndrome. It will be important to determine whether other uncharacterized forms of muscular dystrophy are caused by defects in other glycosyltransferases, such as galactosyltransferase and sialyltransferase. In the future, α-DG may be a target of new glycotherapeutic strategies for muscular dystrophy as well as for neuronal migration disorder.

In view of the potential importance of this form of glycosylation for a number of developmental and neurobiological processes, the ability to assay vertebrate *O*-mannosyltransferase activity and knowledge of the requirement of a heterodimeric complex for enzyme activity should greatly facilitate progress in the identification and localization of *O*-mannosylated proteins and the elucidation of their functional roles.

This study was supported by Research Grants for Nervous and Mental Disorders (14B-4) and Research on Psychiatric and Neurological Diseases and Mental Health from the Ministry of Health, Labour, and Welfare of Japan; by a Grant-in-Aid for Scientific Research on Priority Area (no. 14082209) from the Ministry of Education, Culture, Sports, Science, and Technology of Japan; and by grants from the Mitsubishi Foundation and the Yamanouchi Foundation for Research on Metabolic Disorders.

1. Burton, E. A. & Davies, K. E. (2002) *Cell* **108,** 5–8.
2. Emery, A. E. (2002) *Lancet* **359,** 687–695.
3. Muntoni, F., Brockington, M., Blake, D. J., Torelli, S. & Brown, S. C. (2002) *Lancet* **360,** 1419–1421.
4. Michele, D. E. & Campbell, K. P. (2003) *J. Biol. Chem.* **278,** 15457–15460.
5. Holt, K. H., Crosbie, R. H., Venzke, D. P. & Campbell, K. P. (2000) *FEBS Lett.* **468,** 79–83.
6. Winder, S. J. (2001) *Trends. Biochem. Sci.* **26,** 118–124.
7. Montanaro, F. & Carbonetto, S. (2003) *Neuron* **37,** 193–196.
8. Michele, D. E., Barresi, R., Kanagawa, M., Saito, F., Cohn, R. D., Satz, J. S., Dollar, J., Nishino, I., Kelley, R. I., Somer, H., *et al.* (2002) *Nature* **418,** 417–422.
9. Chiba, A., Matsumura, K., Yamada, H., Inazu, T., Shimizu, T., Kusunoki, S., Kanazawa, I., Kobata, A. & Endo, T. (1997) *J. Biol. Chem.* **272,** 2156–2162.
10. Finne, J., Krusius, T., Margolis, R. K. & Margolis, R. U. (1979) *J. Biol. Chem.* **254,** 10295–10300.
11. Krusius, T., Finne, J., Margolis, R. K. & Margolis, R. U. (1986) *J. Biol. Chem.* **261,** 8237–8242.
12. Krusius, T., Reinhold, V. N., Margolis, R. K. & Margolis, R. U. (1987) *Biochem. J.* **245,** 229–234.
13. Yuen, C. T., Chai, W., Loveless, R. W., Lawson, A. M., Margolis, R. U. & Feizi, T. (1997) *J. Biol. Chem.* **272,** 8924–8931.
14. Sasaki, T., Yamada, H., Matsumura, K., Shimizu, T., Kobata, A. & Endo, T. (1998) *Biochim. Biophys. Acta* **1425,** 599–606.
15. Smalheiser, N. R., Haslam, S. M., Sutton-Smith, M., Morris, H. R. & Dell, A. (1998) *J. Biol. Chem.* **273,** 23698–23703.
16. Chai, W., Yuen, C. T., Kogelberg, H., Carruthers, R. A., Margolis, R. U., Feizi, T. & Lawson, A. M. (1999) *Eur. J. Biochem.* **263,** 879–888.
17. Endo, T. (1999) *Biochim. Biophys. Acta* **1473,** 237–246.
18. Santavuori, P., Somer, H., Sainio, K., Rapola, J., Kruus, S., Nikitin, T., Ketonen, L. & Leisti, J. (1989) *Brain Dev.* **11,** 147–153.
19. Yoshida, A., Kobayashi, K., Manya, H., Taniguchi, K., Kano, H., Mizuno, M., Inazu, T., Mitsuhashi, H., Takahashi, S., Takeuchi, M., *et al.* (2001) *Dev. Cell* **1,** 717–724.
20. Taniguchi, K., Kobayashi, K., Saito, K., Yamanouchi, H., Ohnuma, A., Hayashi, Y. K., Manya, H., Jin, D. K., Lee, M., Parano, E., *et al.* (2003) *Hum. Mol. Genet.* **12,** 527–534.
21. Manya, H., Sakai, K., Kobayashi, K., Taniguchi, K., Kawakita, M., Toda, T. & Endo, T. (2003) *Biochem. Biophys. Res. Commun.* **306,** 93–97.
22. Fukuyama, Y., Osawa, M. & Suzuki, H. (1981) *Brain Dev.* **3,** 1–29.
23. Dobyns, W. B., Pagon, R. A., Armstrong, D., Curry, C. J., Greenberg, F., Grix, A., Holmes, L. B., Laxova, R., Michels, V. V., Robinow, M., *et al.* (1989) *Am. J. Med. Genet.* **32,** 195–210.
24. Kobayashi, K., Nakahori, Y., Miyake, M., Matsumura, K., Kondo-Iida, E., Nomura, Y., Segawa, M., Yoshioka, M., Saito, K., Osawa, M., *et al.* (1998) *Nature* **394,** 388–392.
25. Beltran-Valero De Bernabe, D., Currier, S., Steinbrecher, A., Celli, J., Van Beusekom, E., Van Der Zwaag, B., Kayserili, H., Merlini, L., Chitayat, D., Dobyns, W. B., *et al.* (2002) *Am. J. Hum. Genet.* **71,** 1033–1043.
26. Jurado, L. A., Coloma, A. & Cruces, J. (1999) *Genomics* **58,** 171–180.
27. Strahl-Bolsinger, S., Gentzsch, M. & Tanner, W. (1999) *Biochim. Biophys. Acta* **1426,** 297–307.
28. Aravind, L. & Koonin, E. V. (1999) *Curr. Biol.* **9,** R836–R837.
29. Willer, T., Amselgruber, W., Deutzmann, R. & Strahl, S. (2002) *Glycobiology* **12,** 771–783.
30. Ibraghimov-Beskrovnaya, O., Ervasti, J. M., Leveille, C. J., Slaughter, C. A., Sernett, S. W. & Campbell, K. P. (1992) *Nature* **355,** 696–702.
31. Gentzsch, M. & Tanner, W. (1997) *Glycobiology* **7,** 481–486.
32. Bause, E. & Lehle, L. (1979) *Eur. J. Biochem.* **101,** 531–540.
33. Taniguchi, N., Honke, K. & Fukuda, M. (2002) *Handbook of Glycosyltransferases and Related Genes* (Springer, Tokyo).
34. Gentzsch, M. & Tanner, W. (1996) *EMBO J.* **15,** 5752–5759.
35. Gentzsch, M., Immervoll, T. & Tanner, W. (1995) *FEBS Lett.* **377,** 128–130.
36. Girrbach, V. & Strahl, S. (2003) *J. Biol. Chem.* **278,** 12554–12562.
37. Cormand, B., Pihko, H., Bayes, M., Valanne, L., Santavuori, P., Talim, B., Gershoni-Baruch, R., Ahmad, A., van Bokhoven, H., Brunner, H. G., *et al.* (2001) *Neurology* **56,** 1059–1069.
38. Martin-Blanco, E. & Garcia-Bellido, A. (1996) *Proc. Natl. Acad. Sci. USA* **93,** 6048–6052.
39. Kano, H., Kobayashi, K., Herrmann, R., Tachikawa, M., Manya, H., Nishino, I., Nonaka, I., Straub, V., Talim, B., Voit, T., *et al.* (2002) *Biochem. Biophys. Res. Commun.* **291,** 1283–1286.
40. Hayashi, Y. K., Ogawa, M., Tagawa, K., Noguchi, S., Ishihara, T., Nonaka, I. & Arahata, K. (2001) *Neurology* **57,** 115–121.
41. Brockington, M., Blake, D. J., Prandini, P., Brown, S. C., Torelli, S., Benson, M. A., Ponting, C. P., Estournet, B., Romero, N. B., Mercuri, E., *et al.* (2001) *Am. J. Hum. Genet.* **69,** 1198–1209.
42. Grewal, P. K., Holzfeind, P. J., Bittner, R. E. & Hewitt, J. E. (2001) *Nat. Genet.* **28,** 151–154.
43. Esapa, C. T., Benson, M. A., Schroder, J. E., Martin-Rendon, E., Brockington, M., Brown, S. C., Muntoni, F., Kroger, S. & Blake, D. J. (2002) *Hum. Mol. Genet.* **11,** 3319–3331.

PERGAMON

Neuromuscular Disorders 15 (2005) 336–341

www.elsevier.com/locate/nmd

Proteolysis of β-dystroglycan in muscular diseases

Kiichiro Matsumura[a,*], Di Zhong[a], Fumiaki Saito[a], Ken Arai[a], Katsuhito Adachi[b], Hisaomi Kawai[c], Itsuro Higuchi[d], Ichizo Nishino[e], Teruo Shimizu[a]

[a]*Department of Neurology and Neuroscience, Teikyo University School of Medicine,2-11-1 Kaga Itabashi-ku, Tokyo 173-8605, Japan*
[b]*Department of Internal Medicine, Tokushima National Hospital, 1354 Shikiji, Kamojima-cho, Oe-gun, Tokushima 776-8585, Japan*
[c]*Takamatsu Municipal Hospital,2-36-1 Miyawaki-cho, Takamatsu, Kagawa 760-8538, Japan*
[d]*Third Department of Internal, Medicine, Kagoshima University of Graduate School of Medical and Dental Sciences, 8-35-1 Sakuragaoka, Kagoshima, Kagoshima 890-8544, Japan*
[e]*Department of Neuromuscular, Research, National Institute of Neuroscience, 4-1-1 Ogawahigashi-cho, Kodaira, Tokyo187-8502, Japan*

Received 22 November 2004; received in revised form 5 January 2005; accepted 11 January 2005

Abstract

α-Dystroglycan is a cell surface peripheral membrane protein which binds to the extracellular matrix (ECM), while β-dystroglycan is a type I integral membrane protein which anchors α-dystroglycan to the cell membrane via the N-terminal extracellular domain. The complex composed of α-and β-dystroglycan is called the dystroglycan complex. We reported previously a matrix metalloproteinase (MMP) activity that disrupts the dystroglycan complex by cleaving the extracellular domain of β-dystroglycan. This MMP creates a characteristic 30 kDa fragment of β-dystroglycan that is detected by the monoclonal antibody 43DAG/8D5 directed against the C-terminus of β-dystroglycan. We also reported that the 30 kDa fragment of β-dystroglycan was increased in the skeletal and cardiac muscles of cardiomyopathic hamsters, the model animals of sarcoglycanopathy, and that this resulted in the disruption of the link between the ECM and cell membrane via the dystroglycan complex. In this study, we investigated the proteolysis of β-dystroglycan in the biopsied skeletal muscles of various human muscular diseases, including sarcoglycanopathy, Duchenne muscular dystrophy (DMD), Becker muscular dystrophy, Fukuyama congenital muscular dystrophy, Miyoshi myopathy, LGMD2A, facioscapulohumeral muscular dystrophy, myotonic dystrophy and dermatomyositis/polymyositis. We show that the 30 kDa fragment of β-dystroglycan is increased significantly in sarcoglycanopathy and DMD, but not in the other diseases. We propose that the proteolysis of β-dystroglycan may contribute to skeletal muscle degeneration by disrupting the link between the ECM and cell membrane in sarcoglycanopathy and DMD.

Keywords: Dystroglycan; Sarcoglyan; Dystrophin; Laminin; Extracellular matrix; Matrix metalloproteinase; Sarcoglycanopathy; Duchenne muscular dystrophy

1. Introduction

The dystroglycan complex is a cell membrane-spanning complex composed of α-and β-dystroglycan, which are encoded by a single gene *Dag1* and cleaved into two proteins by posttranslational processing [1]. α-Dystroglycan is a cell surface peripheral membrane protein which binds to laminin in the basement membrane, while β-dystroglycan is a type I integral membrane protein which anchors α-dystroglycan to the cell membrane via the N-terminus of the extracellular domain and binds to the cytoskeletal protein dystrophin via the C-terminal cytoplasmic domain [1–5]. Thus, the dystroglycan complex provides a tight link between the extracellular matrix (ECM) and intracellular cytoskeleton. Recently, we reported a matrix metalloproteinase (MMP) activity that disrupts the dystroglycan complex by cleaving the extracellular domain of β-dystroglycan specifically [6]. This MMP creates a characteristic 30 kDa fragment of β-dystroglycan (β-DG_{30}) that is detected by the monoclonal antibody 43DAG/8D5 directed against the C-terminus of β-dystroglycan [6].

In the previous study, we showed that β-DG_{30} was increased in the skeletal and cardiac muscles of cardiomyopathic hamsters [7], the model animals of sarcoglycanopathy (SGCP) [8,9], and that this resulted in the disruption of the link

* Corresponding author. Tel.: +81 3 3964 1211x1915; fax: +81 3 3964 6394.
E-mail address: k-matsu@med.teikyo-u.ac.jp (K. Matsumura).

0960-8966/$ - see front matter © 2005 Elsevier B.V. All rights reserved.
doi:10.1016/j.nmd.2005.01.007

between the ECM and cell membrane via the dystroglycan complex in these tissues [7]. In the present study, we investigated the proteolysis of β-dystroglycan in the biopsied skeletal muscles of various human muscular diseases. We show that β-DG_{30} is increased significantly in SGCP and Duchenne muscular dystrophy (DMD), but not in the other diseases.

2. Materials and methods

2.1. Patients

Tables 1 and 2 summarize the patients investigated in this study. The skeletal muscle specimens were obtained by diagnostic biopsy. The diseases include SGCP, DMD, Becker muscular dystrophy (BMD), Fukuyama congenital muscular dystrophy (FCMD), Miyoshi myopathy (MM), LGMD2A, facioscapulohumeral muscular dystrophy (FSHD), myotonic dystrophy (DM) and dermatomyositis/

Table 1
Summary of the patients and results of immunoblot analysis of β-dystroglycan in the skeletal muscle biopsy specimens

Diagnosis	No.	Age	Sex	β-DG_{30}/β-DG_{full}	Average±SE
Normal control	1	13	M	0.0358	0.0538±0.0165
	2	14	M	0.0496	
	3	15	M	0.0411	
	4	15	M	0.0127	
	5	16	M	0.0823	
	6	40	M	0.0228	
	7	41	M	0.0253	
	8	43	F	0.0125	
	9	59	M	0.0687	
	10	62	M	0.1869	
SGCP	1	10M	F	2.1467	0.6801±0.2299
	2	7	F	0.3227	
	3	8	M	0.2978	
	4	13	F	0.6819	
	5	15	F	1.0325	
	6	17	F	0.2721	
	7	18	F	0.2500	
	8	31	F	0.4374	
DMD	1	4M	M	0.3729	0.4540±0.0944
	2	1	M	0.4553	
	3	1	M	0.4868	
	4	3	M	0.6436	
	5	3	M	0.3541	
	6	4	M	0.4800	
	7	4Y10M	M	0.3303	
	8	5	M	0.3762	
	9	5	M	0.5457	
	10	6	M	0.5272	
	11	7Y1M	M	0.5011	
	12	8Y9M	M	0.3745	
BMD	1	3	M	0.0309	0.1030±0.0253
	2	3Y10M	M	0.1340	
	3	4Y7M	M	0.0585	
	4	5	M	0.1236	
	5	13	M	0.1681	
FCMD	1	7M	F	0.0218	0.0336±0.0069
	2	8M	F	0.0213	
	3	9M	M	0.0599	
	4	9M	M	0.0421	
	5	9M	M	0.0204	
	6	1Y	F	0.0166	
	7	1Y5M	F	0.0658	
	8	3Y	F	0.0209	
MM	1	25	F	0.0991	0.0779±0.0164
	2	27	M	0.0652	
	3	30	M	0.1313	
	4	38	M	0.0504	
	5	39	M	0.0436	
LGMD2A	1	7Y3M	F	0.0752	0.0646±0.0148
	2	11	F	0.0794	
	3	20	M	0.0206	
	4	26	F	0.0832	
FSHD	1	8	M	0.1307	0.1048±0.0234
	2	19	F	0.0966	
	3	25	M	0.1363	
	4	41	M	0.0170	
	5	48	M	0.1437	
DM	1	14	M	0.0652	0.0722±0.0226
	2	28	M	0.0701	
	3	37	F	0.1541	
	4	50	F	0.0557	
	5	60	M	0.0161	
DM/PM	1	2Y5m	M	0.0762	0.0589±0.0135
	2	3	F	0.0951	
	3	4	F	0.0602	
	4	4	M	0.0000	
	5	10	F	0.1340	
	6	23	M	0.0168	
	7	30	F	0.0114	
	8	33	F	0.0477	
	9	46	M	0.0512	
	10	51	F	0.0957	

The skeletal muscle biopsy specimens were analyzed by immunoblotting using the monoclonal antibody 43DAG/8D5 and the β-DG_{30}/β-DG_{full} ratio was obtained for each patient as described in Materials and Methods. SE, standard error.

Table 2
Genetic analysis of SGCP patients

Patient no	Genetic analysis
1	β-SG, 325 C to T (R109X), homozygous
2	β-SG, 325 C to T (R109X), homozygous
3	α-SG, 229 C to T (R77C), homozygous
4	γ-SG, 630-702 base deletion, homozygous
5	Not done
6	α-SG, 229 C to T (R77C), homozygous
7	α-SG, 220 C to T (R74W), homozygous
8	α-SG, 410 A to G (E137G)/409-423 bases insertion

Patient 5 was diagnosed as SGCP, based on the clinical profile and the specific deficiency of the components of the sarcoglycan complex in the biopsied skeletal muscle as revealed by immunohistochemical analysis (not shown).

polymyositis (DM/PM). The diagnoses were made based on the clinical features, histochemical and immunohistochemical analyses of skeletal muscle biopsy specimens. Genetic diagnoses were also made in some cases. The patients with no obvious pathological changes in the skeletal muscle specimens were included as normal controls.

2.2. *Immunoblot analysis of β-dystroglycan in the biopsied skeletal muscles*

The skeletal muscle specimens were extracted quickly by homogenizing and boiling in a buffer containing 80 mM Tris-HCl, pH 6.8, 10% SDS, 1% β-mercaptoethanol and 115 mM sucrose, in the presence of protease inhibitors, including 0.6 mg/ml pepstatin A, 0.5 mg/ml aprotinin, 0.5 mg/ml leupeptin, 1 mM benzamidine, 1 mM PMSF, 1 mM EDTA, 1 mM EGTA and 20 mg/ml N-Biphenylsulfonyl-phenylalanine hydroxamic acid (a kind gift from Shionogi & Co. Ltd), as described previously [6,7,10]. 3–15% SDS-polyacrylamide gel electrophoresis and immunoblotting were performed as described previously [6,7,10]. The proteolysis of β-dystroglycan was detected by the monoclonal antibody 43DAG/8D5 against the C-terminus of β-dystroglycan (a kind gift from Dr L. V. B. Anderson of Newcastle General Hospital) [6,7,11]. Immunoblot development was done by enhanced chemiluminescence (Pierce) and visualized by Image Station 440 system (Eastman Kodak Company, New Haven, CT). The band intensity of β-DG_{30} and the full-size 43 kDa β-dystroglycan (β-DG_{full}) was measured using 1D image analyzing software and the ratio of β-DG_{30} against β-DG_{full} (β-DG_{30}/β-DG_{full} ratio) was calculated for each patient. The average value of the β-DG_{30}/β-DG_{full} ratio was obtained for normal control and various muscular diseases. The statistical difference among the groups was first tested using one factor ANOVA and then the difference between normal control and each disease group was evaluated by Dunnett's analysis.

3. Results

The results are summarized in Table 1 and Fig. 1. The actual immunoblots of some of the patients are shown in Fig. 2. Although there was some variation among patients, a 30 kDa band corresponding to β-DG_{30} was clearly observed in all the patients with SGCP and DMD (Table 1 and Fig. 2). Statistical analysis demonstrated significant increase of the β-DG_{30}/β-DG_{full} ratio in SGCP and DMD, compared to normal control (Table 1 and Fig. 1). On the other hand, statistical analysis did not demonstrate significant increase of the β-DG_{30}/β-DG_{full} ratio in BMD, FCMD, MM, LGMD2A, FSHD, DM and DM/PM, compared to normal control (Table 1 and Fig. 1), although mild proteolysis was detectable in some individuals (Table 1 and Fig. 2).

We performed the histochemical analysis of skeletal muscle biopsy specimens in order to see if pathological changes were correlated with the increase of proteolysis of β-dystroglycan. The severity of the pathological changes

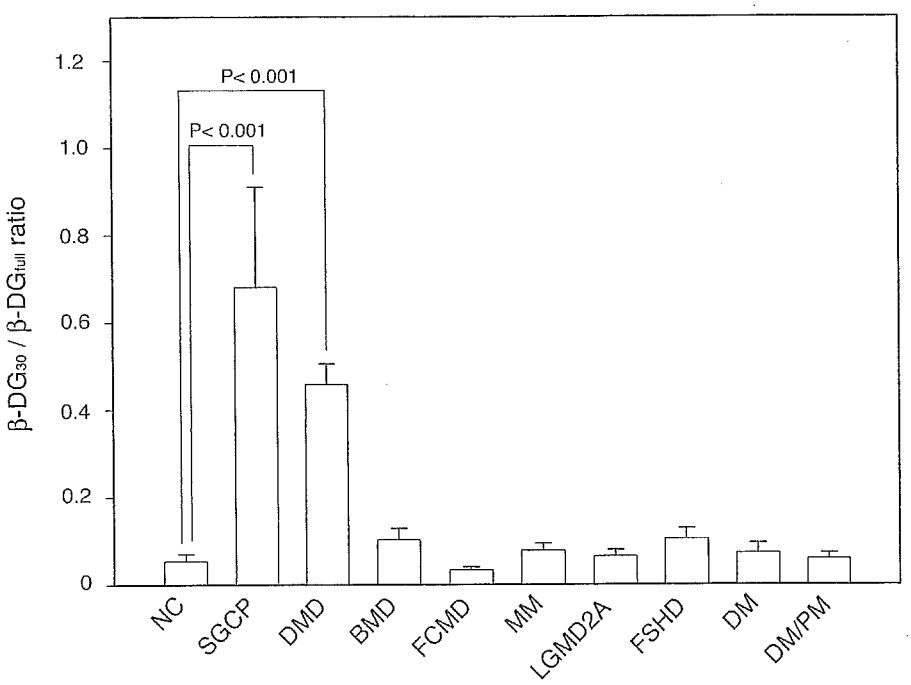

Fig. 1. The ratio of β-DG_{30} against β-DG_{full} in various muscular diseases.The average value of the β-DG_{30}/β-DG_{full} ratio was obtained for normal control and various muscular diseases. The statistical difference among the groups was first tested using one factor ANOVA and then the difference between normal control and each disease group was evaluated by Dunnett's analysis. The β-DG_{30}/β-DG_{full} ratio was significantly increased in SGCP ($P<0.001$) and DMD ($P<0.05$), compared to normal control. There was no significant difference between other disease groups and normal control. Error bar indicates standard error.

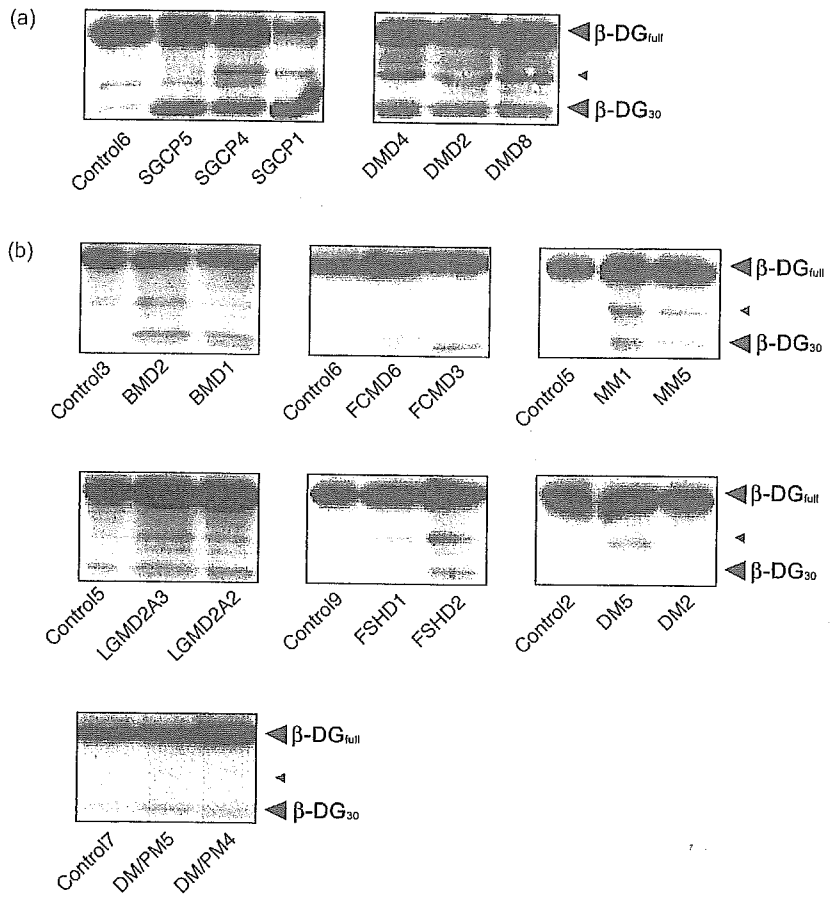

Fig. 2. Immunoblot analysis of β-dystroglycan in the skeletal muscle biopsy specimens of various muscular diseases.The skeletal muscle biopsy specimens were analyzed by immunoblotting using the monoclonal antibody 43DAG/8D5. SGCP and DMD are shown in (a) and BMD, FCMD, MM, LGMD2A, FSHD, DM and DM/PM are shown in (b). Except DMD, equal amount of proteins were loaded for each lane, using myosin heavy chain as internal standard as described previously [10]. For DMD, approximately three times volume of normal control was loaded to visualize β-dystroglycan which is severely reduced in this disease [17]. The band indicated by the small a nrrowhead corresponds to what we reported previously as the intermediate proteolytic fragment of β-DG_{full} [6,7].

was variable not only among the different disease groups but also among the patients with the same disease (Fig. 3). Overall, however, necrotic muscle fibers were observed most frequently in DM/PM, and less frequently in DMD, SGCP and MM (Fig. 3). Hypercontracted muscle fibers were observed most frequently in DMD and SGCP, and less frequently in BMD, DM/PM and FCMD (Fig. 3). Necrotic and hypercontracted muscle fibers were observed infrequently in the other diseases (Fig. 3). Interstitial fibrosis and infiltration of inflammatory cells were mostprominent in FCMD and DM/PM, respectively (Fig. 3).

4. Discussion

Disruption of the tight linkage between the ECM and cell membrane provided by the dystroglycan complex is presumed to have a deleterious effect on the stability of sarcolemma and viability of muscle cells [2,3,6]. Several mechanisms are conceivable that disrupt this linkage. One is the defective glycosylation of β-dystroglycan, which has been demonstrated in several forms of severe congenital muscular dystrophies [for review, see 12–15]. In these diseases, primary defects of the genes encoding the putative glycosyltransferases disturb the glycosylation of β-dystroglycan crucial for the binding of laminin [16] and result in the disruption of the ECM-cell membrane linkage via the dystroglycan complex [12–15]. Recent evidence indicates that the interaction of a glycosyltransferase LARGE with the N-terminal domain of β-dystroglycan is necessary to initiate the posttranslational glycosylation within the mucin domain of β-dystroglycan [17]. The MMP activity that cleaves the extracellular domain of β-dystroglycan is another mechanism that can disrupt this linkage [6]. In the previous study, we showed that this MMP activity was activated in the skeletal and cardiac muscles of cardiomyopathic hamsters, the model animals of SGCP, resulting in the disruption of the dystroglycan complex [7]. Importantly, we showed that this phenomenon was not an in vitro artifact but rather occurred in vivo [7].

In this study, we investigated the proteolysis of β-dystroglycan in the biopsied skeletal muscles of various

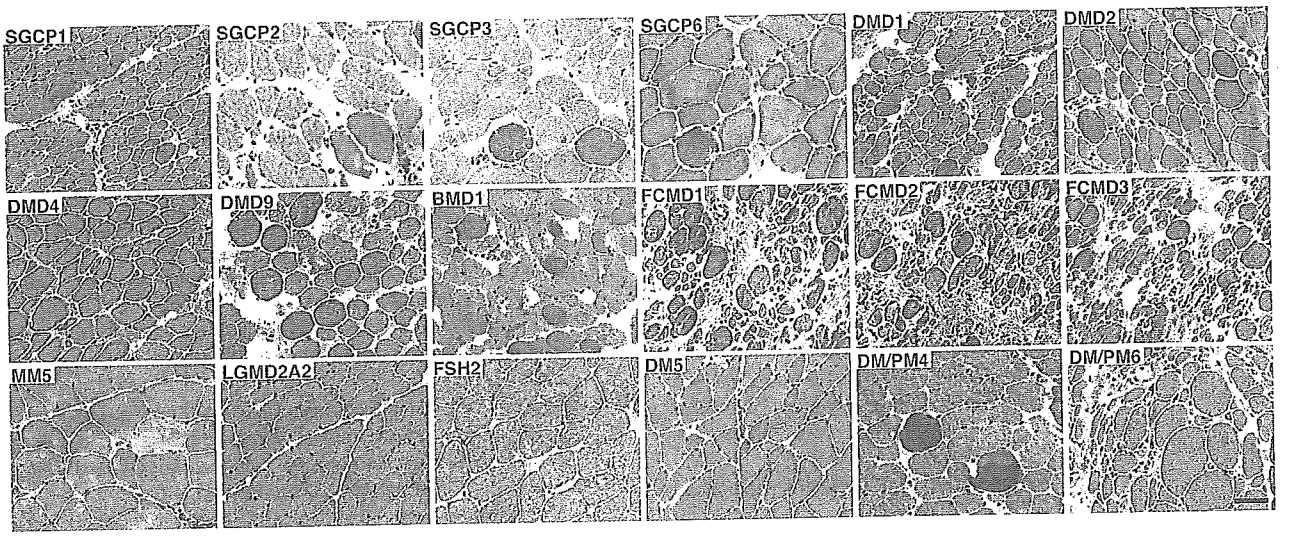

Fig. 3. Histochemical analysis of the skeletal muscle biopsy specimens.The skeletal muscle biopsy specimens were analyzed by staining with hematoxylin and eosin. The severity of the pathological changes was variable not only among the different disease groups but also among the patients with the same disease. Overall, necrotic muscle fibers were observed most frequently in DM/PM, and less frequently in DMD, SGCP and MM. Hypercontracted muscle fibers were observed most frequently in DMD and SGCP, and less frequently in BMD, DM/PM and FCMD. Necrotic and hypercontracted muscle fibers were infrequently observed in the other diseases. Interstitial fibrosis and infiltration of inflammatory cells were most prominent in FCMD and DM/PM, respectively. Bar, 50 μm.

human muscular diseases. We found that the proteolysis of β-dystroglycan was increased significantly in SGCP and DMD. The present results confirm the previous observation by Anderson and Davison, who referred to a similar phenomenon in the biopsied skeletal muscles of SGCP patients [11]. However, they attributed this to the artificial degradation and did not present the results in details [11]. Together with the aforementioned results in cardiomyopathic hamsters [7], we propose that the proteolysis of β-dystroglycan in SGCP is not an in vitro artifact but rather occurs in vivo. On the other hand, this study is the first to report the increased proteolysis of β-dystroglycan in DMD.

At present, the mechanism by which the proteolysis of β-dystroglycan is increased in SGCP and DMD remains obscure. In this respect, it should be noted that hypercontracted muscle fibers were observed frequently in the patients with SGCP and DMD, raising a possibility that the proteolysis of β-dystroglycan may reflect the active degeneration process of muscle fibers. However, the proteolysis of β-dystroglycan was not severe in the patients with BMD and DM/PM who had numerous hypercontracted muscle fibers (for instance, BMD1 and DM/PM4 of Fig. 3). These results suggest that other or additional mechanisms may be present that contribute to the proteolysis of β-dystroglycan. For instance, it is possible that the deficiency of the sarcoglycan complex may render β-dystroglycan susceptible to proteolysis, because it is well established that the sarcoglycan complex is specifically and drastically reduced in these two diseases [18]. In any case, the resulting proteolysis of β-dystroglycan will disrupt the link between the ECM and cell membrane via the dystroglycan complex and render muscle fibers susceptible to further degeneration.

The proteolysis of β-dystroglycan was not significantly increased in BMD, FCMD, MM, LGMD2A, FSHD, DM and DM/PM, although mild proteolysis was detectable in some individuals. When we initiated this study, we were particularly interested if the proteolysis of β-dystroglycan by MMP was activated in FCMD. In FCMD skeletal muscle, the glycosylation of β-dystroglycan crucial for the binding of laminin is disturbed, resulting in the disruption of the ECM-cell membrane linkage via the dystroglycan complex [19]. We wondered if this might render β-dystroglycan susceptible to proteolysis but have found that this is not the case in this study. We also wondered if the proteolysis of β-dystroglycan was increased in DM/PM, because various MMPs are reported activated in inflammatory myopathies [20–22]. However, this did not turn out to be the case in this study. Our results suggest that the MMP that cleaves the extracellular domain of β-dystroglycan may be distinct from those reported activated in inflammatory myopathies.

Acknowledgements

We thank Miki Yamanaka and Yuka Sasayama for their expert technical assistance. This work was supported by [1] Research Grants 14B-4 and 16B-1 for Nervous and Mental Disorders (Ministry of Health, Labor and Welfare), [2] Research on Psychiatric and Neurological Diseases and Mental Health (Ministry of Health, Labor and Welfare), and [3] Research Grant 16390256 and 'High-Tech Research Center' Project for Private Universities: matching fund subsidy from MEXT (Ministry of Education, Culture, Sports, Science and Technology), 2004–2008.

References

[1] Ibraghimov-Beskrovnaya O, Ervasti JM, Leveille CJ, Slaughter CA, Sernett SW, Campbell KP. Primary structure of dystrophin-associated glycoproteins linking dystrophin to the extracellular matrix. Nature 1992;355:696–702.

[2] Henry MD, Campbell KP. Dystroglycan: an extracellular matrix receptor linked to the cytoskeleton. Curr Opin Cell Biol 1996;8:625–31.

[3] Winder SJ. The complexities of dystroglycan. Trends Biochem Sci 2001;26:118–24.

[4] Stasio ED, Sciandra F, Maras B, et al. Structural and functional analysis of the N-terminal extracellular region of β-dystroglycan. Biochem Biophys Res Comm 1999;206:274–8.

[5] Ishikawa-Sakurai M, Yoshida M, Imamura M, Davies KE, Ozawa E. ZZ domain is essentially required for the physiological binding of dystrophin and utrophin to β-dystroglycan. Hum Molec Genet 2004; 13:693–702.

[6] Yamada H, Saito F, Fukuta-Ohi H, et al. Processing of β-dystroglycan by matrix metalloproteinase disrupts the link between the extracellular matrix and cell membrane via the dystroglycan complex. Hum Molec Genet 2001;10:1563–9.

[7] Matsumura K, Arai K, Zhong D, et al. Disruption of dystroglycan axis by β-dystroglycan processing in cardiomyopathic hamster muscle. Neuromusc Disord 2003;13:796–803.

[8] Nigro V, Okazaki Y, Belsito A, et al. Identification of the Syrian hamster cardiomyopathy gene. Hum Molec Genet 1997; 6:601–7.

[9] Sakamoto A, Ono K, Abe M, et al. Both hypertrophic and dilated cardiomyopathies are caused by mutation of the same gene, δ-sarcoglycan, in hamster: an animal model of disrupted dystrophin-associated glycoprotein complex. Proc Natl Acad Sci USA 1997;94: 13873–8.

[10] Matsumura K, Tome FMS, Collin H, et al. Deficiency of the 50K dystrophin-associated glycoprotein in severe childhood autosomal recessive muscular dystrophy. Nature 1992;359:320–2.

[11] Anderson LVB, Davison K. Multiplex western blotting system for the analysis of muscular dystrophy patients. Am J Pathol 1999;154: 1017–22.

[12] Martin-Rendon E, Blake DJ. Protein glycosylation in disease: new insights into the congenital muscular dystrophies. Trends Pharmacol Sci 2003;24:178–83.

[13] Grewal PK, Hewitt JE. Glycosylation defects: a new mechanism for muscular dystrophy? Hum Molec Genet 2003;12: 259–64.

[14] Endo T, Toda T. Glycosylation in congenital muscular dystrophies. Biol Pharm Bull 2003;26:1641–7.

[15] Muntoni F, Brockington M, Torelli S, Brown SC. Defective glycosylation in congenital muscular dystrophies. Curr Opin Neurol 2004;17:205–9.

[16] Chiba A, Matsumura K, Yamada H, et al. Structures of sialylated O-linked oligosaccharides of bovine peripheral nerve α-dystroglycan: the role of a novel mannosyl type oligosaccharide in the binding with laminin. J Biol Chem 1997;272:2156–62.

[17] Kanagawa M, Saito F, Kunz S, et al. Molecular recognition by LARGE is essential for expression of functional dystroglycan. Cell 2004;117:953–64.

[18] Ohlendieck K, Matsumura K, Ionasescu VV, et al. Duchenne muscular dystrophy: deficiency of dystrophin-associated proteins in the sarcolemma. Neurology 1993;43:795–800.

[19] Michele DE, Barresi R, Kanagawa M, et al. Post-translational disruption of dystroglycan–ligand interactions in congenital muscular dystrophies. Nature 2002;418:417–22.

[20] Choi YC, Dalakas MC. Expression of matrix metalloproteinases in the muscle of patients with inflammatory myopathies. Neurology 2000; 54:65–71.

[21] Kieseier BC, Schneider C, Clements JM, et al. Expression of specific matrix metalloproteinases in inflammatory myopathies. Brain 2001; 124:341–51.

[22] Schoser BG, Blottner D, Stuerenburg HJ. Matrix metalloproteinases in inflammatory myopathies: enhanced immunoreactivity near atrophic myofibers. Acta Neurol Scand 2002;105:309–13.

FEBS 29463

FEBS Letters 579 (2005) 2359–2363

Aberrant glycosylation of α-dystroglycan causes defective binding of laminin in the muscle of chicken muscular dystrophy

Fumiaki Saito[a,*], Martina Blank[b], Jörn Schröder[b], Hiroshi Manya[c], Teruo Shimizu[a], Kevin P. Campbell[d], Tamao Endo[c], Makoto Mizutani[e], Stephan Kröger[b], Kiichiro Matsumura[a]

[a] *Department of Neurology and Neuroscience, Teikyo University, 2-11-1 Kaga, Itabashi-ku, Tokyo 173-8605, Japan*
[b] *Institute for Physiological Chemistry, University of Mainz, Duesbergweg 6, D-55099 Mainz, Germany*
[c] *Glycobiology Research Group, Tokyo Metropolitan Institute of Gerontology, 35-2 Sakae-chyo, Itabashi-ku, Tokyo 173-0015, Japan*
[d] *Howard Hughes Medical Institute, Department of Physiology and Biophysics and Department of Neurology, The University of Iowa, Roy J. and Lucille A. Carver College of Medicine, 400 Eckstein medical research building, Iowa City, IA 52242-1101, USA*
[e] *Nippon Institute for Biological Science, 3331-114 kamisasao, kobuchisawa-chyo, Yamanashi prefecture 408-0041, Japan*

Received 17 February 2005; revised 9 March 2005; accepted 9 March 2005

Available online 25 March 2005

Edited by Sandro Sonnino

Abstract **Dystroglycan is a central component of dystrophin–glycoprotein complex that links extracellular matrix and cytoskeleton in skeletal muscle. Although dystrophic chicken is well established as an animal model of human muscular dystrophy, the pathomechanism leading to muscular degeneration remains unknown. We show here that glycosylation and laminin-binding activity of α-dystroglycan (α-DG) are defective in dystrophic chicken. Extensive glycan structural analysis reveals that Galβ1-3GalNAc and GalNAc residues are increased while Siaα2-3Gal structure is reduced in α-DG of dystrophic chicken. These results implicate aberrant glycosylation of α-DG in the pathogenesis of muscular degeneration in this model animal of muscular dystrophy.**

Keywords: Dystroglycan; Laminin; Muscular dystrophy; Glycosylation; Dystrophic chicken

1. Introduction

The dystroglycan complex is composed of two proteins, α- and β-dystroglycan (α- and β-DG), which are encoded by a single gene and cleaved by posttranslational processing [1]. α-DG is a highly glycosylated extracellular peripheral membrane protein and binds to several extracellular matrix (ECM) proteins including laminin, agrin, and perlecan [2–4]. In turn, the transmembrane protein β-DG anchors α-DG at the extracellular surface of the plasma membrane, while its cytoplasmic domain interacts with dystrophin, a large cytoplasmic protein that binds to F-actin [5]. Thus, the DG complex plays a crucial role to stabilize the plasma membrane by acting as an axis through which the ECM is tightly linked to the cytoskeleton.

Recently, primary mutations in the genes encoding putative glycosyltransferases have been identified in several types of congenital muscular dystrophies including Fukuyama-type congenital muscular dystrophy, muscle–eye–brain disease, Walker–Warburg syndrome, congenital muscular dystrophy 1C (MDC1C) and 1D (MDC1D) [6–10]. Because glycosylation and laminin-binding activity of α-DG are defective in these diseases [11], they are collectively called α-dystroglycanopathy [12]. However, the precise oligosaccharide structures defective in α-dystroglycanopathy have not been elucidated.

Muscular dystrophy in chicken was first described in 1956 [13]. Although dystrophic chicken has been established as an animal model of muscular dystrophy, the primary mutation has not yet been identified [14] and the pathomechanism leading to muscle cell degeneration remains unknown. We demonstrate here that glycosylation and laminin-binding activity of α-DG are defective in the skeletal muscle of dystrophic chicken. Extensive glycan structural analysis reveals that, compared to control chicken, the amount of Galβ1-3GalNAc and GalNAc residues are increased, whereas Siaα2-3Gal structure is reduced in α-DG of dystrophic chicken.

2. Materials and methods

2.1. Antibodies

Mouse monoclonal antibody against sugar chain moiety of α-DG (IIH6) and sheep polyclonal antibody against core protein of α-DG (sheep anti-α-DG) were described previously [2,15]. Mouse monoclonal antibody against sugar chain moiety of α-DG (IVA4-1) was obtained from Upstate Biotechnology. Mouse monoclonal antibody against β-DG (8D5), β-sarcoglycan (5B1) and γ-sarcoglycan (21B5) were kind gifts from Dr. L.V.B. Anderson (Newcastle General Hospital). Mouse monoclonal anti-dystrophin (MANDRA 1) and affinity isolated rabbit anti-laminin were obtained from Sigma. Mouse monoclonal anti-dystrobrevin was purchased from BD Biosciences.

2.2. Lectin chromatography

Dystrophic chicken used in this study is New Hampshire, line 413, the colony of which is maintained homozygously. Line GSN/1, was used as a control. Pectoralis muscle of dystrophic and control chicken of 3 months of age were used. Skeletal muscle was disrupted with a polytron followed by Daunce homogenization and incubation in 50 mM Tris–HCl, pH 7.4, 500 mM NaCl, 1% Triton X-100, 0.6 μg/ml pepstatin A, 0.5 μg/ml leupeptin, 0.5 μg/ml aprotinin, 0.75 mM benzamidine, and 0.1 mM PMSF. The extract was incubated with lectin

*Corresponding author. Fax: +813 3964 6394.
E-mail address: f-saito@med.teikyo-u.ac.jp (F. Saito).

Abbreviations: DG, dystroglycan; DGC, dystrophin–glycoprotein complex

0014-5793/$30.00
doi:10.1016/j.febslet.2005.03.033

agarose, including wheat germ agglutinin (WGA), concanavalin A (Con A), peanut agglutinin (PNA), *Vicia villosa* agglutinin isolectin B_4 (VVA-B_4), *Maackia amurensis* lectin (MAM) and lentil lectin (LCA). Bound proteins were eluted by boiling the beads in sample buffer (65 mM Tris–HCl, pH 6.9, 3% SDS, 1% β-mercaptoethanol, 115 mM sucrose, and 0.0004% bromophenol blue) and the eluates were analyzed by Western blotting using sheep anti-α-DG.

2.3. Miscellaneous

Chemical deglycosylation was described previously [2]. Sialidase digestion was performed using sialidase from *Clostridium perfringens* (Roche) according to the procedure described elsewhere [16]. Immunofluorescent microscopic analysis, Western blotting and blot overlay assay were performed as described elsewhere [11]. The amount of glycosidically bound sialic acid was compared by periodate–resorcinol method [17] and statistical significance was evaluated by *t* test. Solid-phase assay was performed as previously mentioned [11] except that WGA eluates were coated on 96 wells EIA/RIA plates (Coaster) after measuring the band intensity of α-DG on Western blots so that each well contained the same amount of α-DG.

3. Results

3.1. Decreased immunoreactivity of α-DG in the skeletal muscle of dystrophic chicken

We first performed immunofluorescent microscopic analysis. The immunoreactivity of α-DG revealed by antibody against sugar chain moiety of α-DG was significantly decreased in dystrophic chicken, whereas the immunoreactivity of α-DG was indistinguishable between control and dystrophic chicken when detected by antibody against core protein of α-DG. The other components of dystrophin–glycoprotein complex (DGC) were normally expressed in dystrophic chicken (Fig. 1). Consistent with the immunofluorescent analysis, Western blotting with antibody against sugar chain moiety of α-DG demonstrated reduced immunoreactivity of α-DG in dystrophic chicken (Fig. 2). In addition, α-DG of dystrophic chicken migrated at 160 kD, faster than that of control which migrated at 200 kD (Fig. 2). The expression and molecular mass of the other components of the DGC were not altered (Fig. 2).

3.2. Altered glycosylation of α-DG in the skeletal muscle of dystrophic chicken

The results described above raise the possibility that the glycosylation, rather than expression, of α-DG in dystrophic chicken may be altered. In order to test this possibility, α-DG was enriched by WGA chromatography and chemically deglycosylated with trifluoromethanesulfonic acid. Similar to the antibody against sugar chain moiety of α-DG, antibody against core protein of α-DG recognized α-DG species migrating around 200 and 160 kD in control and dystrophic chicken, respectively (Fig. 3, deglycosylation −). In addition, however, the anti-core protein antibody also detected α-DG species with a lower molecular mass of 110 kD in control and 70–120 kD in dystrophic chicken (Fig. 3, deglycosylation −). In this report, we tentatively call the larger and smaller α-DG species as L-α-dystroglycan (L-α-DG) and S-α-dystroglycan (S-α-DG), respectively. Upon chemical deglycosylation, the molecular mass of α-DG was reduced to 55 kD both in control and dystrophic chicken equally, eliminating the difference in molecular mass (Fig. 3, deglycosylation +). These data indicate that α-DG is aberrantly glycosylated in the skeletal muscle of dystrophic chicken. We also examined various tissues of dystrophic chicken to see if defective glycosylation of α-DG was present. Western blot analysis using antibody against core protein of α-DG demonstrated a

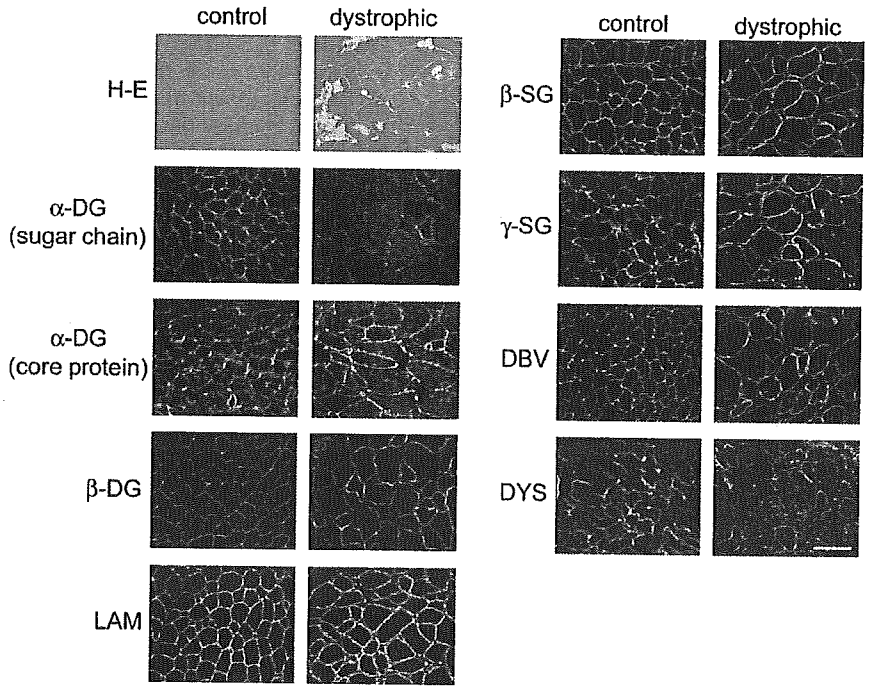

Fig. 1. Immunoreactivity of α-dystroglycan is reduced in the skeletal muscle of dystrophic chicken when probed by antibody against sugar chain moiety. Expression and localization of each component of the DGC were analyzed by immunofluorescent microscopy. The immunoreactivity of α-DG, as revealed by antibody against sugar chain moiety of α-DG (IIH6), is reduced in dystrophic chicken. However, the expression of α-DG core protein is not altered. DG, dystroglycan; LAM, laminin; SG, sarcoglycan; DBV, dystrobrevin; DYS, dystrophin. Bar indicates 100 μm.

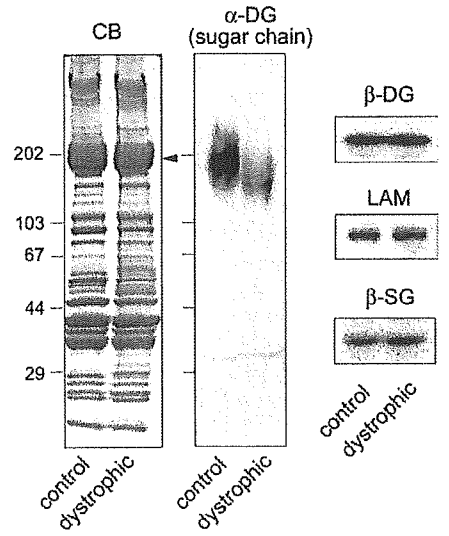

Fig. 2. The molecular mass of α-DG is decreased in the skeletal muscle of dystrophic chicken. Western blotting was performed to examine the expression of α-DG using whole skeletal muscle homogenates. The amount of protein loaded for each lane was normalized using myosin heavy chain as internal standard (arrowhead in the panel CB). α-DG in dystrophic chicken migrates faster than that in control and the immunoreactivity of α-DG is decreased in dystrophic chicken using antibody against sugar chain moiety of α-DG (IIH6). The expression of other components of the DGC is not altered. CB, Coomassie blue staining; DG, dystroglycan; LAM, laminin; SG, sarcoglycan.

downward shift in the molecular mass of α-DG in cardiac muscle, but not in other tissues including brain, peripheral nerve, kidney, spleen and liver (data not shown), indicating

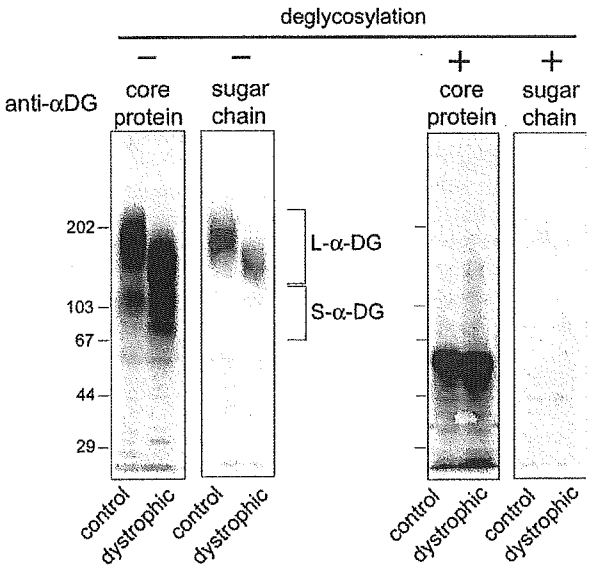

Fig. 3. Deglycosylation eliminates the difference in molecular mass of α-DG between control and dystrophic chicken. α-DG was enriched by WGA chromatography and chemically deglycosylated with trifluoromethanesulfonic acid. Antibody against core protein of α-DG recognizes α-DG species with higher molecular mass (L-α-DG), which are also detected by antibody against sugar chain moiety of α-DG (VIA4-1). In addition, the anti-core protein of α-DG recognizes α-DG species with lower molecular mass (S-α-DG). After deglycosylation, the molecular mass of α-DG decreases to 55 kD in both control and dystrophic chicken equally (deglycosylation +).

that glycosylation of α-DG was also altered in the cardiac muscle of dystrophic chicken.

3.3. Laminin-binding activity of α-DG is decreased in the skeletal muscle of dystrophic chicken

Blot overlay assays demonstrated that the binding of laminin 1 and 2 to α-DG was greatly reduced in dystrophic chicken (Fig. 4A). Notably, both laminin 1 and 2 bound to L-α-DG, but not S-α-DG (Fig. 4A). The band intensity of S-α-DG and L-α-DG was measured and the ratio of S-α-DG against total α-DG (intensity of S-α-DG/intensity of S-α-DG + L-α-DG) was calculated. The ratio of S-α-DG was 16.8 ± 4.5% in control versus 40.9 ± 4.1% in dystrophic chicken (Fig. 4B), indicating that many more α-DG molecules in dystrophic chicken lack the laminin-binding activity than control. Next, we performed quantitative solid-phase assay. The total laminin-binding activity was significantly decreased in the skeletal muscle of dystrophic chicken (Fig. 4C).

3.4. Glycosylation defects of dystrophic chicken α-DG analyzed by lectin chromatography

To investigate the change in glycan structure of α-DG in dystrophic chicken, we performed a set of lectin chromatographies.

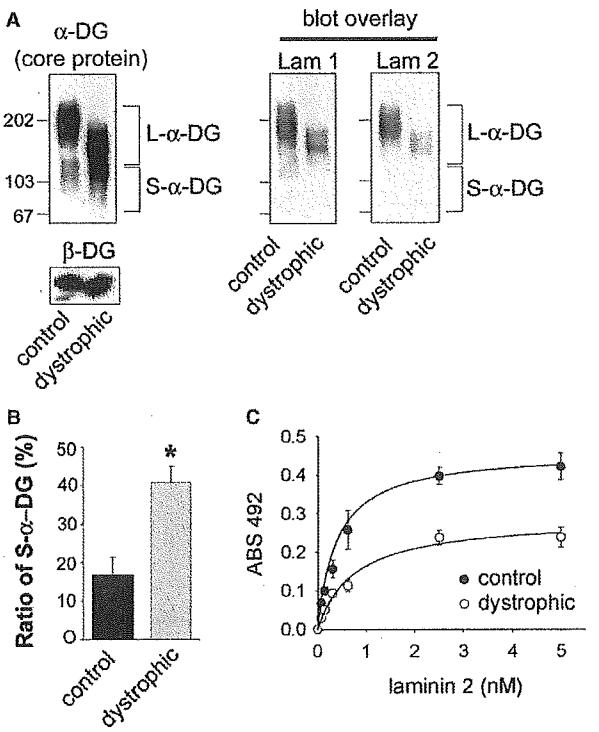

Fig. 4. Laminin-binding activity of α-DG is decreased in the skeletal muscle of dystrophic chicken. (A) Equal amount of DG was transferred to PVDF membranes as revealed by Western blotting for α-DG and β-DG. Blot overlay assays demonstrate that the binding of both laminin 1 and 2 to α-DG is substantially decreased in dystrophic chicken. Both laminin 1 and 2 bind to L-α-DG, but not S-α-DG. Lam 1, laminin 1; Lam 2, laminin 2. (B) The band intensity of L-α-DG and S-α-DG was measured and the ratio of S-α-DG against total α-DG was calculated. The ratio of S-α-DG is significantly higher in dystrophic chicken. $^{*}P < 0.003$. (C) Solid-phase assay reveals that laminin-binding activity is significantly reduced in the skeletal muscle of dystrophic chicken.

As shown in Fig. 5A, Con A bound most of the α-DG species, whereas LCA had no significant interaction with any α-DG species (Fig. 5A). In sharp contrast, MAM bound L-α-DG in control, while it interacted only weakly with α-DG in dystrophic chicken (Fig. 5A), indicating that Siaα2-3Gal moieties are profoundly reduced in α-DG of dystrophic chicken. Interestingly, PNA bound to a fraction of S-α-DG in dystrophic chicken, while no binding to α-DG occurred in control (Fig. 5B, sialidase −). VVA-B_4 bound weakly to S-α-DG in control, whereas it strongly interacted with L-α-DG and S-α-DG in dystrophic chicken. Because the reactivity of these lectins are known to be severely decreased when sialic acids are attached to non-reducing termini of their binding sugar chain moieties [18], we enzymatically removed sialic acids by sialidase and repeated the experiments. After sialidase digestion, both S-α-DG and L-α-DG extensively interacted with PNA in dystrophic chicken, whereas only a small amount of S-α-DG was recovered in control. These results indicate that Galβ1-3GalNAc moieties are much more abundant on α-DG in dystrophic chicken than that in control (Fig. 5B, sialidase +). Similar result was obtained with VVA-B_4, indicating that GalNAc structures are much more abundant on α-DG of dystrophic chicken (Fig. 5B, sialidase +). The amount of glycosidically bound sialic acids quantified by periodate–resorcinol method was substantially reduced in dystrophic chicken (Fig. 5C), which is consistent with the result of MAM lectin chromatography.

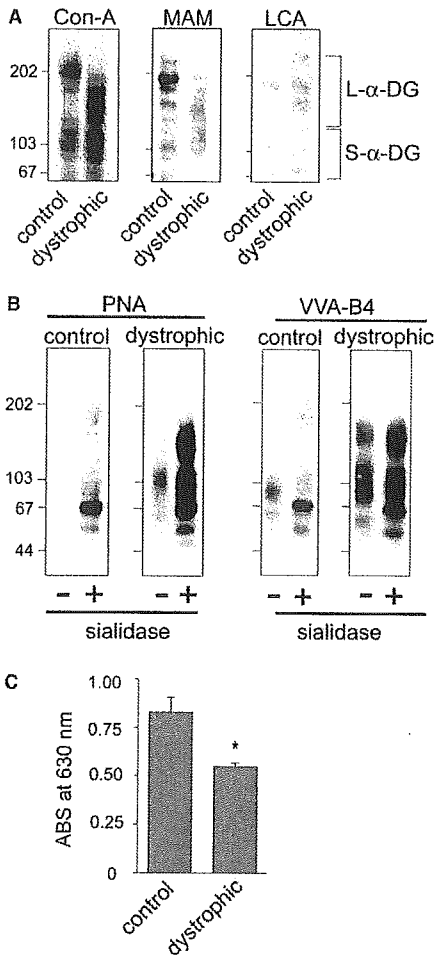

Fig. 5. Glycosylation of α-DG is altered in the skeletal muscle of dystrophic chicken. (A) α-DG was extracted using Triton X-100 and applied to lectin chromatography. The bound α-DG was visualized by Western blotting using antibody against core protein of α-DG. Con-A binds most of the α-DG species, while LCA does not interact with any α-DG species significantly. MAM strongly binds only to L-α-DG in control. (B) The Triton X-100 extracts were applied to PNA or VVA-B_4 chromatography with or without prior digestion by sialidase. Without sialidase treatment, PNA binds S-α-DG in dystrophic chicken, while it does not interact with α-DG in control (sialidase −). VVA-B_4 binds S-α-DG in control only weakly, while it interacts strongly with both L- and S-α-DG in dystrophic chicken (sialidase −). With sialidase digestion, both PNA and VVA-B_4 bind extensively to L-α-DG and S-α-DG in dystrophic chicken compared to control (sialidase +). (C) Quantification of sialic acid by periodate–resorcinol method reveals that the amount of glycosidically bound sialic acids in the skeletal muscle of dystrophic chicken is significantly less than that of control chicken. $^*P < 0.001$.

4. Discussion

The mucin-like domain of α-DG is heavily glycosylated by *O*-linked glycans [19], with the sugar chain moieties constituting up to two-thirds of its total molecular mass [1,2]. The antibody against sugar chain moiety of α-DG detected only L-α-DG, while anti-α-DG core protein detected both L-α-DG and S-α-DG (Figs. 2 and 3), indicating diverse glycosylation of α-DG in vivo. Notably, laminin bound to L-α-DG, but not to S-α-DG, in both control and dystrophic chicken (Fig. 4), indicating that the interaction of laminin with α-DG is strictly regulated through glycosylation of α-DG and that a fraction of α-DG does not possess the sugar chain moieties necessary for the binding of laminin in vivo. Furthermore, the ratio of non-laminin-binding α-DG (S-α-DG) is greatly increased in dystrophic chicken compared to control (Fig. 4). It would be intriguing to postulate that the increase of non-laminin-binding α-DG may contribute to the dystrophic phenotype by exerting a dominant negative effect in dystrophic chicken, where non-laminin-binding α-DG competes with laminin-binding α-DG for the cytoskeletal linkage via dystrophin. Consistent with this hypothesis, we have observed that adenovirus mediated gene transfer of non-laminin-binding α-DG constructs results in the degeneration of skeletal muscle in mice (Saito and Campbell, unpublished observation).

The results of lectin chromatography indicate that, compared to control chicken, the amount of Galβ1-3GalNAc and GalNAc residues are increased significantly while Siaα2-3Gal structure is severely decreased in α-DG of dystrophic chicken (Fig. 5). The reduction in the amount of sialic acids was confirmed by periodate–resorcinol sialic acid assay (Fig. 5). However, α-DG appears to be hyposialylated rather than asialylated (Fig. 5C). We have reported recently that hyposialylation of α-DG alone is not enough to abolish its laminin-binding activity in vivo [20]. It remains to be determined if hyposialylation in dystrophic chicken reflects the reduction of the sialyl *O*-mannosyl glycan, Sia2-3Galβ1-4GlcNAcβ1-2Man-Ser/Thr, implicated in the binding of laminin [21,22].

Pavoni et al. [23] reported recently that antibody against C-terminal portion of α-DG core protein detected α-DG with molecular mass of 109 kD in the skeletal muscle of normal chicken. Our S-α-DG may correspond to this small α-DG, as judged by molecular mass. Pavoni et al. further postulated that this 109 kD α-DG might be a partially glycosylated form of

α-DG. In the present study, we provided clear evidence of actual alteration of glycosylation of this small α-DG molecule (Figs. 3 and 5). The molecular mass of α-DG in the skeletal muscle of normal chicken was reported to change during development [24]. It would be thus interesting to see if the molecular mass of α-DG in the skeletal muscle of dystrophic chicken also changes during development by future studies.

In conclusion, we have demonstrated altered glycosylation and decreased laminin-binding activity of α-DG in chicken muscular dystrophy. Furthermore, we have demonstrated that Siaα2-3Gal structure is reduced, while Galβ1-3GalNAc and GalNAc moieties are increased on α-DG of this animal model of muscular dystrophy. These data would contribute to further understand the molecular mechanism of muscular degeneration caused by disturbed glycosylation of α-DG in human muscular dystrophies.

Acknowledgments: We thank Hiroko F. Ohi, Miki Yamanaka and Yuka Sasayama for their expert technical assistance. This work was supported by [1] Research Grants 14B-4 and 16B-1 for Nervous and Mental Disorders (Ministry of Health, Labor and Welfare), [2] Research on Psychiatric and Neurological Diseases and Mental Health (Ministry of Health, Labor and Welfare), [3] Research Grant 16390256 and "High-Tech Research Center" Project for Private Universities: matching fund subsidy from MEXT (Ministry of Education, Culture, Sports, Science and Technology), 2004–2008, and [4] a research grant from the Ichiro Kanahara Foundation.

References

[1] Ibraghimov-Beskrovnaya, O., Ervasti, J.M., Leveille, C.J., Slaughter, C.A., Sernett, S.W. and Campbell, K.P. (1992) Primary structure of dystrophin-associated glycoproteins linking dystrophin to the extracellular matrix. Nature 355, 696–702.

[2] Ervasti, J.M. and Campbell, K.P. (1993) A role for the dystrophin–glycoprotein complex as a transmembrane linker between laminin and actin. J. Cell. Biol. 122, 809–823.

[3] Bowe, M.A., Deyst, K.A., Leszyk, J.D. and Fallon, J.R. (1994) Identification and purification of an agrin receptor from Torpedo postsynaptic membranes: a heteromeric complex related to the dystroglycans. Neuron 12, 1173–1180.

[4] Peng, H.B., Ali, A.A., Daggett, D.F., Rauvala, H., Hassell, J.R. and Smalheiser, N.R. (1998) The relationship between perlecan and dystroglycan and its implication in the formation of the neuromuscular junction. Cell Adhes. Commun. 5, 475–489.

[5] Jung, D., Yang, B., Meyer, J., Chamberlain, J.S. and Campbell, K.P. (1995) Identification and characterization of the dystrophin anchoring site on β-dystroglycan. J. Biol. Chem. 270, 27305–27310.

[6] Kobayashi, K., Nakahori, Y., Miyake, M., Matsumura, K., Kondo-Iida, E., Nomura, Y., Segawa, M., Yoshioka, M., Saito, K., Osawa, M., Hamano, K., Sakakihara, Y., Nonaka, I., Nakagome, Y., Kanazawa, I., Nakamura, Y., Tokunaga, K. and Toda, T. (1998) An ancient retrotransposal insertion causes Fukuyama-type congenital muscular dystrophy. Nature 394, 388–392.

[7] Yoshida, A., Kobayashi, K., Manya, H., Taniguchi, K., Kano, H., Mizuno, M., Inazu, T., Mitsuhashi, H., Takahashi, S., Takeuchi, M., Herrmann, R., Straub, V., Talim, B., Voit, T., Topaloglu, H., Toda, T. and Endo, T. (2001) Muscular dystrophy and neuronal migration disorder caused by mutations in a glycosyltransferase, POMGnT1. Dev. Cell 1, 717–724.

[8] Beltran-Valero De Bernabe, D., Currier, S., Steinbrecher, A., Celli, J., Van Beusekom, E., Van Der Zwaag, B., Kayserili, H., Merlini, L., Chitayat, D., Dobyns, W.B., Cormand, B., Lehesjoki, A.E., Cruces, J., Voit, T., Walsh, C.A., van Bokhoven, H. and Brunner, H.G. (2002) Mutations in the *O*-mannosyltransferase gene POMT1 give rise to the severe neuronal migration disorder Walker–Warburg syndrome. Am. J. Hum. Genet. 71, 1033–1043.

[9] Brockington, M., Blake, D.J., Prandini, P., Brown, S.C., Torelli, S., Benson, M.A., Ponting, C.P., Estournet, B., Romero, N.B., Mercuri, E., Voit, T., Sewry, C.A., Guicheney, P. and Muntoni, F. (2001) Mutations in the fukutin-related protein gene (FKRP) cause a form of congenital muscular dystrophy with secondary laminin α2 deficiency and abnormal glycosylation of α-dystroglycan. Am. J. Hum. Genet. 69, 1198–1209.

[10] Longman, C., Brockington, M., Torelli, S., Jimenez-Mallebrera, C., Kennedy, C., Khalil, N., Feng, L., Saran, R.K., Voit, T., Merlini, L., Sewry, C.A., Brown, S.C. and Muntoni, F. (2003) Mutations in the human LARGE gene cause MDC1D, a novel form of congenital muscular dystrophy with severe mental retardation and abnormal glycosylation of α-dystroglycan. Hum. Mol. Genet. 12, 2853–2861.

[11] Michele, D.E., Barresi, R., Kanagawa, M., Saito, F., Cohn, R.D., Satz, J.S., Dollar, J., Nishino, I., Kelley, R.I., Somer, H., Straub, V., Mathews, K.D., Moore, S.A. and Campbell, K.P. (2002) Posttranslational disruption of dystroglycan–ligand interactions in congenital muscular dystrophies. Nature 418, 417–422.

[12] Michele, D.E. and Campbell, K.P. (2003) Dystrophin–glycoprotein complex: post-translational processing and dystroglycan function. J. Biol. Chem. 278, 15457–15460.

[13] Asmundson, V.S. and Julian, L.M. (1956) Inherited muscle abnormalityin the domestic fowl. J. Hered. 47, 248–252.

[14] Lee, E.J., Yoshizawa, K., Mannen, H., Kikuchi, H., Kikuchi, T., Mizutani, M. and Tsuji, S. (2002) Localization of the muscular dystrophy AM locus using a chicken linkage map constructed with the Kobe University resource family. Anim. Genet. 33, 42–48.

[15] Herrmann, R., Straub, V., Blank, M., Kutzick, C., Franke, N., Jacob, E.N., Lenard, H.G., Kroger, S. and Voit, T. (2000) Dissociation of the dystroglycan complex in caveolin-3-deficient limb girdlemuscular dystrophy. Hum. Mol. Genet. 9, 2335–2340.

[16] Yamada, H., Chiba, A., Endo, T., Kobata, A., Anderson, L.V., Hori, H., Fukuta-Ohi, H., Kanazawa, I., Campbell, K.P., Shimizu, T. and Matsumura, K. (1996) Characterization of dystroglycan–laminin interaction in peripheral nerve. J. Neurochem. 66, 1518–1524.

[17] Jourdian, G.W., Dean, L. and Roseman, S. (1971) The sialic acids. XI. A periodate–resorcinol method for the quantitative estimation of free sialic acids and their glycosides. J. Biol. Chem. 246, 430–435.

[18] Ervasti, J.M., Burwell, A.L. and Geissler, A.L. (1997) Tissue-specific heterogeneity in α-dystroglycan sialoglycosylation. Skeletal muscle α-dystroglycan is a latent receptor for *Vicia villosa* agglutinin B4 masked by sialic acid modification. J. Biol. Chem. 272, 22315–22321.

[19] Brancaccio, A., Schulthess, T., Gesemann, M. and Engel, J. (1995) Electron microscopic evidence for a mucin-like region in chick muscle α-dystroglycan. FEBS Lett. 368, 139–142.

[20] Saito, F., Tomimitsu, H., Arai, K., Nakai, S., Kanda, T., Shimizu, T., Mizusawa, H. and Matsumura, K. (2004) A Japanese patient with distal myopathy with rimmed vacuoles: Missense mutations in the epimerase domain of the UDP-*N*-acetylglucosamine 2-epimerase/*N*-acetylmannosamine kinase (GNE) gene accompanied by hyposialylation of skeletal muscle glycoproteins. Neuromuscul. Disord. 14, 158–161.

[21] Chiba, A., Matsumura, K., Yamada, H., Inazu, T., Shimizu, T., Kusunoki, S., Kanazawa, I., Kobata, A. and Endo, T. (1997) Structures of sialylated *O*-linked oligosaccharides of bovine peripheral nerve α-dystroglycan. J. Biol. Chem. 272, 2156–2162.

[22] Sasaki, T., Yamada, H., Matsumura, K., Shimizu, T., Kobata, A. and Endo, T. (1998) Detection of *O*-mannosyl glycans in rabbit skeletal muscle α-dystroglycan. Biochim. Biophys. Acta 1425, 599–606.

[23] Pavoni, E., Sciandra, F., Barca, S., Giardina, B., Petrucci, T.C. and Brancaccio, A. (2005) Immunodetection of partially glycosylated isoforms of α-dystroglycan by a new monoclonal antibody against its β-dystroglycan-binding epitope. FEBS Lett. 579, 493–499.

[24] Leschziner, A., Moukhles, H., Lindenbaum, M., Gee, S.H., Butterworth, J., Campbell, K.P. and Carbonetto, S. (2000) Neural regulation of α-dystroglycan biosynthesis and glycosylation in skeletal muscle. J. Neurochem. 74, 70–80.

ELSEVIER

Neurobiology of Disease

www.elsevier.com/locate/ynbdi
Neurobiology of Disease 19 (2005) 208–217

Basement membrane fragility underlies embryonic lethality in *fukutin*-null mice

Hiroki Kurahashi,[a,b] Mariko Taniguchi,[a] Chikara Meno,[c] Yoshihiro Taniguchi,[d] Satoshi Takeda,[d] Masato Horie,[d] Hiroki Otani,[e] and Tatsushi Toda[a,*]

[a]*Division of Functional Genomics, Department of Post-Genomics and Diseases, Osaka University Graduate School of Medicine, 2-2-B9 Yamadaoka, Suita, Osaka 565-0871, Japan*
[b]*Division of Molecular Genetics, Institute for Comprehensive Medical Science, Fujita Health University, Toyoake, Aichi 470-1192, Japan*
[c]*Developmental Genetics Group, Osaka University Graduate School of Frontier Biosciences, Suita, Osaka 565-0871, Japan*
[d]*Otsuka GEN Research Institute, Otsuka Pharmaceutical Co. Ltd., Tokushima 771-0192, Japan*
[e]*Department of Developmental Biology, Faculty of Medicine, Shimane University, Izumo, Shimane 693-8501, Japan*

Received 12 October 2004; revised 17 December 2004; accepted 28 December 2004
Available online 19 February 2005

Fukuyama-type congenital muscular dystrophy (FCMD), associated with brain malformation due to defects in neuronal migration, is caused by mutations in *fukutin*. Several lines of evidence suggest that the fukutin protein plays a pivotal role in synthesis of *O*-mannosyl sugar moieties of α-dystroglycan, a cell surface laminin receptor. Here, through targeted disruption of the orthologous mouse *fukutin* gene, we show that the fukutin protein is essential, as homozygous-null embryos die by E9.5 of gestation. *Fukutin*-null embryos show phenotypic diversity, features of which include growth retardation, folding of the egg cylinder, leakage of maternal red blood cells into the yolk sac cavity, and an increased number of apoptotic cells in the ectoderm. Loss of immunoreactivity against sugar moieties in α-dystroglycan suggests a reduced laminin-binding capacity. Ultrastructural analysis shows thin and breached basement membranes (BMs). BM fragility may underlie all of these abnormal phenotypes, and maintenance of BM function may require fukutin-mediated glycosylation of α-dystroglycan early in embryonic development.

Keywords: fukutin; α-Dystroglycan; Basement membrane

Introduction

Dystroglycan is a key component of the dystrophin–glycoprotein complex (DGC), linking intracellular dystrophin with proteins in the extracellular matrix (Michele and Campbell, 2003). It is composed of α and β subunits (α-DG and β-DG), which are encoded as a single protein by *DAG1* and posttranslationally cleaved. The extracellular α-DG and transmembrane β-DG both undergo extensive glycosylation and form heterodimers. Although mutations in genes encoding DGC proteins are known to be involved in muscular dystrophies, disease-related mutations in dystroglycan itself have not been identified. In mice, targeted disruption of the *DAG1* gene results in embryonic lethality, indicating an essential role for dystroglycan in organizing basement membranes (BMs) during early embryogenesis (Henry and Campbell, 1998; Williamson et al., 1997).

Evidence is accumulating to suggest that abnormal glycosylation of α-DG underlies muscular dystrophies. The mutation responsible for mouse myodystrophy (*myd*) is an intragenic deletion in *Large*, which encodes a putative glycosyltransferase for α-DG (Grewal et al., 2001). Muscle-eye-brain disease (MEB), an autosomal recessive disorder characterized by congenital muscular dystrophy, ocular abnormalities, and lissencephaly, is associated with mutations in the novel glycosyltransferase *O*-mannose β-1,2-*N*-acetylglucosaminyltransferase (POMGnT1) (Yoshida et al., 2001), and examination of muscle tissue from MEB patients has revealed hypoglycosylation of α-DG (Kano et al., 2002; Michele et al., 2002). We have proposed a new clinical entity called α-dystroglycanopathy to reflect the involvement of abnormal α-DG glycosylation in multiple muscular dystrophies (Toda et al., 2003a,b).

Fukuyama-type congenital muscular dystrophy (FCMD; MIM 253800) also belongs to this group of disorders. An autosomal recessive disorder, FCMD is characterized by congenital muscular dystrophy associated with brain malformation due to a defect in neuronal migration. Previously, we identified the gene responsible for FCMD, *fukutin* (Kobayashi et al., 1998; Toda et al., 1993). Most patients with FCMD carry a retrotransposal insertion in the 3′ untranslated region of *fukutin*, an alteration that reduces levels of *fukutin* mRNA transcript. While its function remains unconfirmed, several lines of evidence suggest that the fukutin protein plays a

* Corresponding author. Fax: +81 6 6879 3389.
E-mail address: toda@clgene.med.osaka-u.ac.jp (T. Toda).
Available online on ScienceDirect (www.sciencedirect.com).

0969-9961/$ - see front matter © 2005 Elsevier Inc. All rights reserved.
doi:10.1016/j.nbd.2004.12.018

role in α-DG glycosylation. First, fukutin is a Golgi-resident protein and shares some homology with fringe-like glycosyltransferases (Aravind and Koonin, 1999; Kobayashi et al., 1998). Second, immunoreactivity against the sugar moiety of α-DG is reduced in muscle tissue from FCMD patients (Hayashi et al., 2001). Third, it has recently been demonstrated that hypoglycosylation in FCMD directly abolishes binding of α-DG to the ligands laminin, neurexin, and agrin (Michele et al., 2002; Takeda et al., 2003). Together, these results suggest a functional linkage between fukutin and glycosylation of α-DG.

To study the function of the *fukutin* gene product, we have constructed homozygous-null mice using a gene targeting method. These mice do not survive beyond an early embryonic stage. Analysis of mutant embryos has shown that fukutin plays a pivotal role in maintaining the integrity of the basement membrane (BM). These studies also indicate that multiple BM functions are essential in the developing mouse embryo.

Materials and methods

Targeted disruption of mouse fukutin gene

A cosmid clone spanning exons 1 to 5 of the mouse *fukutin* gene was isolated from a 129/SvEv mouse library (Horie et al., 2002). The targeting vector was constructed with a 12-kb *Kpn*I–*Blp*I fragment containing the first coding exon (exon 2) and flanking introns. The 2.3-kb *Kpn*I–*Bam*HI fragment containing exon 2 was replaced with a neomycin resistance gene (pKO-Select Neo, Lexicon), thereby removing the sequence encoding amino acids 1–35, as well as the splicing donor and acceptor sites (Takeda et al., 2003). Targeting vectors were linearized using *Not*I, and AB2.2 prime ES cells (Lexicon) were electroporated with the neo^r vector. We picked, expanded, and screened Geneticin-resistant (Sigma) clones for homologous recombination. Targeted *fukutin* gene disruption was confirmed by Southern blot analysis of genomic DNA from ES cells (Takeda et al., 2003). The targeted ES cell clone was expanded and injected into E3.5 blastocysts of the C57BL/6 mouse strain using standard methods. Chimeric males were bred with C57BL/6 females to generate heterozygous mice from chimeras transmitting the mutation. The targeted mutation has been maintained in 129/SvEv × C57BL/6 hybrid backgrounds. Mice were maintained in accordance with the Animal Care guidelines of Otsuka Pharmaceutical Co. Ltd.

Genotyping

Embryos were obtained from intercrosses of heterozygotes. Embryos analyzed at E6.5, E7.5, and E8.5 were genotyped by PCR. Staging of embryos was performed according to standard conventions (i.e., E0.5 is 1PM on the day of the copulation plug). Genomic DNA was extracted from yolk sac tissue using standard methods. When samples were prepared from slices, embryonic tissues were obtained using Laser Capture Microdissection (Arcturus), and then DNA was isolated. PCR amplification for genotyping was performed using the following primers: MoE2F (5′-GAAGTATCTCTGGTCACAGG-3′) and MoE1R (5′-ACAGCAGAAAGGCAGAACTC-3′) for exon 2 of the Fcmd gene (Horie et al., 2002); NeoF4 (5′-CGACGTTGTCACTGAAGCG-3′) and NeoR4 (5′-GCTTCCATCCGAGTACGTG-3′) for the neomycin resistance gene, which distinguished mutant from wild type.

Histological analyses

Decidua dissected at E6.5, E7.5, and E8.5 were fixed overnight in 4% paraformaldehyde or Bouin's fixative, and then washed in phosphate-buffered saline (PBS) before dehydration in 25%, 50%, 75%, and 100% ethanol. The tissue was cleared in xylene and embedded in Paraplast (Sigma). Paraffin blocks were sectioned at 5 μm and stained with hematoxylin and eosin.

Immunostaining and fragmented DNA staining

Primary antibodies used in this study include: mouse anti-α-DG monoclonal antibodies (IIH6 and VIA4-1: Upstate Biotechnology); affinity purified rabbit anti-β-DG polyclonal antibody (Imamura et al., 2000); affinity purified rabbit anti-laminin polyclonal antibody (Harber Bio-products); affinity purified rabbit anti-laminin α1 polyclonal antibody; and rabbit anti-collagen IV (LSL). A high-temperature antigen unmasking technique was performed using Antigen Unmasking Solution (Vector Laboratories) prior to staining. For immunostaining, sections were incubated with primary antibodies overnight at 4°C in PBS with 1% goat serum, and then washed three times in PBS. Secondary antibodies labeled with Alexa Fluor 488 (Molecular Probes) or conjugated to HRP (DAKO) were incubated for 1 h at room temperature in PBS with 1% goat serum, followed by three washes in PBS. When using anti-mouse secondary antibodies, the sections were treated with MOM (Vector Laboratories) prior to incubation with primary antibodies to block the endogenous mouse immunoglobulins in the tissue.

Fragmented DNA was detected in paraffin-embedded sections by the TdT-mediated dUTP nick end labeling (TUNEL) method using an in situ cell death detection kit (Roche) according to the manufacturer's instructions. Signals were detected with 3,3′-diaminobenzidine tetrahydrochloride (DAB) before counterstaining with nuclear fast red or methyl green.

In situ hybridization

Whole mount in situ hybridization was performed according to standard protocols. Sense and antisense mouse *fukutin* sequence templates containing T7 or SP6 promoters were created using PCR, and labeled RNA probes were generated by transcribing with T7 or SP6 RNA polymerase and digoxigenin-UTP. For the *Brachyury*, *Hesx1*, *Gata6*, and *Pem* gene probes, plasmids including the appropriate inserts were used as templates for RNA probe transcription (Kispert and Hermann, 1993; Lin et al., 1994; Morrisey et al., 1998; Thomas and Beddington, 1996). For hybridization with *Gata6* and *Pem* probes, embryos were isolated so as not to damage the Reichert's membrane.

Electron microscopy

For electron microscopy, the embryos were fixed with 2% glutaraldehyde, stained with buffered 1% osmium tetroxide, and embedded in epoxy resin. Ultrathin sections (80–90 nm thick) were cut using diamond knives on an Ultracut-E ultramicrotome (Reichert Jung), double-stained with uranyl acetate and lead citrate, and examined under a Hitachi H-7100 electron microscope.

The thickness of the Reichert's membrane was measured using Digital Micrograph 2.1 software. Thickness was measured at three different regions, and a mean thickness was calculated for each embryo.

Results

Fukutin expression during early embryogenesis

Previously, we showed that *fukutin* mRNA is detectable in wild-type E7 embryos, and at E9.5 is present in the neuroepithelium of the forebrain and hindbrain (Horie et al., 2002). Here, we analyzed *fukutin* expression in earlier embryonic stages. In situ hybridization on sections from wild-type embryos showed that *fukutin* is ubiquitously expressed at low levels at E6.5 and E7.5. At E8.5, positive signals were located in neuroepithelium, with weaker signals present in all other tissues (data not shown).

Embryonic lethality in fukutin-null mice

To further investigate the roles of the *fukutin* gene product, we subjected the mouse *fukutin* locus to targeted disruption. A null allele was generated by replacing the first coding exon (exon 2) with a neomycin resistance gene. Since the coding sequence corresponding to amino acids 1–35 is deleted, no functional fukutin protein is expected to be produced from this allele (Takeda et al., 2003).

Mice heterozygous for the *fukutin* mutation appeared grossly normal and were fertile. Genotyping of progeny derived from intercrosses of *fukutin* (+/−) mice showed a complete absence of homozygous-null mutants among the offspring, while heterozygous and wild-type progeny were obtained at the expected ratio of approximately 2:1 (Table 1). This indicates that homozygosity for the *fukutin*-null mutation results in embryonic lethality.

To determine the time of embryonic death, we sacrificed pregnant females from matings between *fukutin* (+/−) mice at different times postcoitum, and the embryos were dissected and genotyped by PCR. The survival rate of homozygous-null embryos decreased gradually during the egg cylinder stage, with no survival observed beyond E9.5 (Table 1).

Phenotypic diversity in fukutin-null embryos

To examine the *fukutin*-null phenotype more closely, we performed histological analysis of decidua sections dissected from the uteri of pregnant females at E6.5, E7.5, and E8.5. After completing the morphological study, we genotyped the embryos by PCR using genomic DNA recovered from the same sections.

Table 1
Genotypes of offspring from heterozygote intercrosses

Age	Number of embryos	Genotype		
		+/+	+/−	−/−
E6.5	19	4	10	5
E7.5	34	5	25	4
E8.5	23	8	13	2
E9.5	60	24	34	2
E10.5	9	2	7	0
E13.5	41	14	27	0
Adult	98	36	62	0

Homozygous-null embryos showed significant phenotypic diversity. At E6.5, some embryos showed striking appearances, with distorted and folded shapes (Fig. 1A). Since the concave face of the folding lacked the Reichert's membrane, the Reichert's membrane itself was not folded; instead, the folded embryo existed within the apparently normal sac of Reichert's membrane. Some folded embryos contained cells with pyknotic nuclei scattered within the epiblast layer (Fig. 1B). The distribution of cells with pyknotic nuclei was random and did not correlate with the direction of the folding.

The first BMs to form during mouse embryonic development are those located between the visceral endoderm and the developing epiblast, and those underneath the parietal endoderm (Reichert's membrane), which extends over the trophoectoderm. Unlike the wild-type embryo, the border between epiblast and endoderm was obscure in homozygous-null E6.5 embryos (Fig. 1B, arrows), indicating a BM defect. Another BM, Reichert's membrane, appeared normal under light microscopic examination. However, maternal red blood cells were detected in the yolk sac cavity in some embryos (Fig. 1B, arrowheads). Since embryos cannot produce red blood cells at this stage, they had presumably entered the yolk sac cavity from the subjacent maternal sinusoids. A small number of homozygous-null E6.5 embryos appeared morphologically indistinguishable from wild-type control littermates (Fig. 1C).

At E7.5, all of the homozygous-null embryos had formed mesoderm and initiated gastrulation. Phenotypic defects continued to be diverse at this stage. Some embryos appeared distorted and folded in shape, and some possessed an obscure border between ectoderm and endoderm (Fig. 1D). The number of cells with pyknotic nuclei increased in some embryos. These embryos were often smaller, with larger extraembryonic portions than embryonic portions (cf. Fig. 2). A small number of embryos appeared grossly normal in shape and could not be distinguished from wild-type control littermates (Fig. 1E).

Analysis of E8.5 embryos revealed no characteristic distortion of the embryo, suggesting that such embryos had been resorbed by this stage. Some mutant embryos were small and disorganized relative to wild-type controls. They appeared to arrest at E7.5, and the process of resorption had been initiated (Fig. 1F). Still, a small number of mutant embryos appeared to be developing normally, albeit with mild growth retardation, having several somites. Even in these morphologically normal embryos, however, cells with pyknotic nuclei were distributed nonspecifically within the neuroectoderm. Reichert's membrane still appeared normal under light microscopic examination (Figs. 1G and H).

We recovered few homozygous-null E9.5 embryos, as most had been resorbed by this stage. They appeared disorganized, although they had developed heart, allantois, and neural plate (data not shown).

Fukutin-null embryo undergoes appropriate differentiation in early embryogenesis

One conceivable explanation for the folding of the embryo is abnormal axial organization. To examine the axial organization of *fukutin*-null embryos, we analyzed the expression patterns of